

Boise State University

ScholarWorks

Geosciences Faculty Publications and
Presentations

Department of Geosciences

8-2024

Palynostratigraphy and Bayesian Age Stratigraphic Model of New CA-ID-TIMS Zircon Ages from the Walloon Coal Measures, Surat Basin, Australia

K. Sobczak

University of Queensland

J. Cooling

University of Queensland

T. Crossingham

University of Queensland

H. G. Holl

University of Queensland

M. Reilly

University of Queensland

See next page for additional authors

Publication Information

Sobczak, K.; Cooling, J.; Crossingham, T.; Holl, H. G.; Reilly, M.; Esterle, J.; . . . and Hurter, S. (2024). "Palynostratigraphy and Bayesian Age Stratigraphic Model of New CA-ID-TIMS Zircon Ages from the Walloon Coal Measures, Surat Basin, Australia". *Gondwana Research*, 132, 150-167. <https://doi.org/10.1016/j.gr.2024.04.012>

Authors

K. Sobczak, J. Cooling, T. Crossingham, H. G. Holl, M. Reilly, J. Esterle, J. L. Crowley, C. Hannaford, M. T. Mohr, Z. Hamerli, and S. Hurter



Contents lists available at ScienceDirect

Gondwana Research

journal homepage: www.elsevier.com/locate/gr

Palynostratigraphy and Bayesian age stratigraphic model of new CA-ID-TIMS zircon ages from the Walloon Coal Measures, Surat Basin, Australia

K. Sobczak^{a,*}, J. Cooling^b, T. Crossingham^a, H.G. Holl^a, M. Reilly^a, J. Esterle^b, J.L. Crowley^c, C. Hannaford^d, M.T. Mohr^c, Z. Hamerli^a, S. Hurter^a

^a Centre for Natural Gas, University of Queensland, Sir James Foots Building (47A), St Lucia QLD 4072, Australia

^b School of the Environment, University of Queensland, Steele Building (3), St Lucia QLD 4072, Australia

^c Department of Geosciences, Boise State University, Boise, ID 83725, USA

^d MGPalaeo, Unit 1, 5 Arvida St, Malaga WA 6090, Australia

ARTICLE INFO

Article history:

Received 21 December 2023

Revised 6 April 2024

Accepted 7 April 2024

Available online 9 May 2024

Handling Editor: Jan Marten Huizenga

Keywords:

U-Pb zircon geochronology

Chronostratigraphy

Palynology

Surat Basin

Walloon Coal Measures

Bayesian age modelling

ABSTRACT

The Surat Basin hosts significant coal and coal seam gas resources. New high-precision CA-TIMS U/Pb zircon ages from tuffs and Bayesian age stratigraphic models are combined with palynology from fine-grained sedimentary rocks and zircon trace elements to provide further chronostratigraphic and biostratigraphic constraints on the Walloon Coal Measures in the eastern margin of the Surat Basin and infer the palaeoenvironment and tectonic setting. The tuff ages range from 165.88 ± 0.11 Ma to 158.84 ± 0.05 Ma, with those from the stratigraphically lower Taroom Coal Measures ranging from 165.88 ± 0.11 to 163.05 ± 0.08 Ma and Juandah Coal Measures ranging from 159.91 ± 0.04 to 158.84 ± 0.05 Ma. This corroborates that the lower part of the Walloon Coal Measures is Callovian and the upper part is Oxfordian. The palynology results from mudstones show that all samples are dominated by microfossils of spore-pollen with conifers being the most abundant. Our samples fall within Price's (1997) stratigraphic zonation of APJ4.2 and APJ4.3. Posterior ages for palynology samples were estimated through Bayesian age stratigraphic modelling using stratigraphic depths and U-Pb zircon ages. The palaeoenvironment in the eastern portion of the basin is inferred to be predominantly fluvial, with spores and pollen derived from fresh water or terrestrial plants. Higher concentrations of green algae in one sample suggest that at times the water was somewhat stagnant. The zircons were derived from predominantly intermediate magmas, as indicated by the generally low Ti, Ta, and Nb values. The tectonic environment that the zircons were derived from was most likely a continental subduction zone due to their high U/Yb, low Nb/Yb and relatively low Hf concentrations. These new data support previous conclusions of the Surat Basin palaeoenvironment, contribute to the ongoing discussion about the tectonic setting of the basin and add new regional age marker horizons.

© 2024 The Authors. Published by Elsevier B.V. on behalf of International Association for Gondwana Research. This is an open access article under the CC BY license (<http://creativecommons.org/licenses/by/4.0/>).

1. Introduction

Regional stratigraphic correlations in the eastern Australian Mesozoic basins are challenging due to the predominance of non-marine depositional environments (e.g., Cook et al., 2013; Green, 1997). In the absence of marine fossils, no reliable biostratigraphic markers exist that can be easily tied to numerical ages. Lithostratigraphic correlations, even on a local scale, are also hindered by complex facies architecture and lateral discontinuity of

lithofacies that is inherent in non-marine depositional settings (e.g., Shanley & McCabe, 1994; Shepherd, 2009).

The stratigraphy of the Surat Basin has traditionally been based on palynological assemblages (Fig. 1). The biostratigraphy of the basin is relatively well-studied thanks to the foundational works of McKellar, Price and others (Fig. 1; e.g., McKellar, 1998; Price, 1997; Price et al., 1985), and some eastern Australian palynological zones have been correlated to global biozones that are more accurately tied to the geologic time scale (de Jersey & McKellar, 2013; Helby et al., 1987; McKellar, 1998). However, a stratigraphic framework solely based on largely uncalibrated palynomorph assemblages creates uncertainty and imprecise correlations.

* Corresponding author.

E-mail address: k.sobczak@uq.edu.au (K. Sobczak).

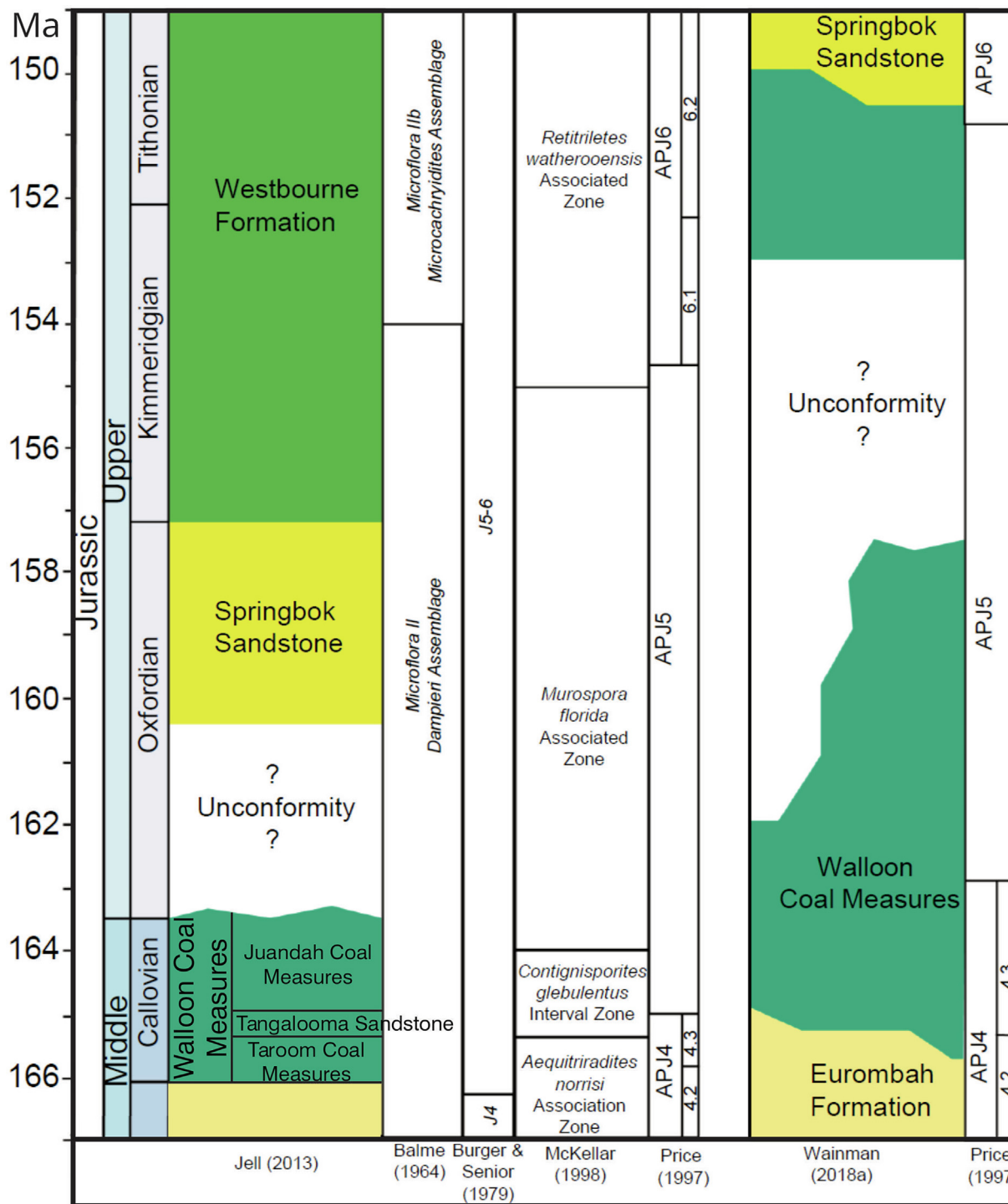


Fig. 1. Partial stratigraphy of the Surat basin modified after Wainman et al., 2018b. The stratigraphic sections include those by Cook et al. (2013) and Wainman et al., (2018b).

Recent chemical abrasion-isotope dilution-thermal ionization mass spectrometry (CA-ID-TIMS) U-Pb zircon geochronology from tuffs and palynostratigraphy studies by Wainman et al., 2015; 2018a; Wainman & McCabe, 2019 have significantly advanced the stratigraphic constraints of the coal-bearing part of the Surat succession, the Walloon Coal Measures, and have improved well-to-well correlations across the northern Surat Basin. The new radioisotopic ages additionally demonstrate that the formation is predominantly Upper Jurassic (Oxfordian–Kimmeridgian; Wainman et al., 2015; 2018a) rather than Middle Jurassic as

previously reported. Additional high-precision geochronology is needed in data-poor areas, as well as for the rest of the Surat Basin formations, whose ages remain poorly constrained. Additionally, continued acquisition of palynological data and refining biozones by linking them to high-precision ages will improve the resolution of temporal constraints in areas where syn-depositional tuffs are absent.

Identifying the petrologic setting the tuffs were derived from can also assist with ongoing discussions about the tectonic mechanism responsible for the formation of the basin. The source of the

syn-depositional volcanism of the tuffs remains disputed, as processes related to the active subduction zone on the eastern margin have been proposed (Gallagher et al., 1994; Green et al., 1997; Henderson et al., 2022; Korsch & Totterdell, 2009a; 2009b; Korsch et al., 2009; Tucker et al., 2016; Waschbusch et al., 2009; Wainman et al., 2015; 2019; Foley et al., 2021; Andrade et al., 2023), as well as intracratonic rifting (Fielding, 1993; Fielding et al., 1996; Martin et al., 2013; Yago and Fielding, 2015; Asmussen et al., 2023). Further investigation of *syn*-depositional zircons could improve the understanding and analysis of the Surat Basin evolution and stratigraphy.

This paper presents new CA-ID-TIMS ages and palynological data from the Walloon Coal Measures, with the aim to improve age constrains and refine the biozones on the eastern margin of the Surat Basin, where few data are available. The new CA-ID-TIMS ages will build on recent chronostratigraphic studies from the basin by adding additional regional markers (Wainman et al., 2015; 2018a; 2019; Wainman & McCabe, 2019). Finally, selected zircon trace element concentrations and ratios will be used as essential information to understand the origin of the tuffs now interspersed in sediment.

2. Geological background

The 300,000 km² Surat Basin is located in south-eastern Queensland and North-eastern New South Wales (Fig. 2; Cook et al., 2013; Raza et al., 2009). It is separated from the time-equivalent Eromanga Basin in the west by the Nebine Ridge, and the Clarence-Moreton Basin in the east by the Kumberilla Ridge (Exon & Senior, 1976; Green et al., 1997). The north–south trending Mimosa Syncline represents the basin's axis (Fig. 2; Exon, 1976).

Approximately 2500 m of sediment was deposited during six fining-upward sedimentary cycles, spanning from the Late Triassic to Early Cretaceous, with strata dipping gently to the southwest (Exon, 1976; Exon & Burger, 1981; Raza et al., 2009). The sediment generally has a terrestrial origin, though it has been suggested that minor marine influences have occurred (Bianchi et al., 2018; Cook

et al., 2013; Exon, 1976; Exon & Burger, 1981; Martin et al., 2018; Raza et al., 2009). Each sedimentary cycle is representative of a transgressive–regressive sequence thought to have been deposited over 10 to 20 Ma (Burke, 2011; Exon, 1976; Hoffmann et al., 2009; La Croix et al., 2020). The focus of this study is the Walloon Coal Measures, which have been interpreted as part of the second sedimentary cycle.

The Walloon Coal Measures are a Middle-Late Jurassic coal-bearing formation within the Surat Basin that continues east into the Clarence-Moreton Basin. In the Surat Basin, the Walloon Coal Measures host the largest coal seam gas reserves in Australia and are therefore a target of intense gas exploration and production (e.g., Ryan et al., 2012; Towler et al., 2016). In the Surat Basin, the formation comprises up to 650 m of fine- to medium-grained lithic sandstones, mudstones, siltstones and coals, with minor ironstone and volcanoclastic rocks (e.g., Exon, 1976; Green et al., 1997; Hamilton et al., 2014; Jones & Patrick, 1981; Power & Devine, 1970; Swarbrick et al., 1973). An overall trend of the coal horizons being more frequent and thicker in the northern parts of the formation with thinning towards the south has been previously recognized (Exon, 1976; Green et al., 1997; Hamilton et al., 2014; Ryan et al., 2012; Scott et al., 2007; Shields & Esterle, 2015; Sliwa & Esterle, 2008; Zhou et al., 2017).

The Walloon Coal Measures have been subdivided in several ways by different authors (e.g., Hamilton et al., 2014; Jones & Patrick, 1982; Scott et al., 2004). The subdivisions include the Juandah (upper) and Taroom (lower) Coal Measures (Hamilton et al., 2014; Jones & Patrick, 1982; Scott et al., 2004). The Tangalooma Sandstone, which is not coal bearing, separates the Juandah and Taroom Coal Measures (Hamilton et al., 2014; Jones & Patrick, 1982; Scott et al., 2004; Fig. 1). As these subdivisions are based on highly variable lithostratigraphy (e.g., Gaede et al., 2020; Sobczak et al., 2021), other means of correlating the units across the basin are required, such as chrono- and biostratigraphy.

Thin (cm- to dm-scale), fine-grained tuff horizons are relatively common throughout this succession (Exon, 1976; Green, 1997). The tuff horizons are discontinuous on a regional scale and, there-

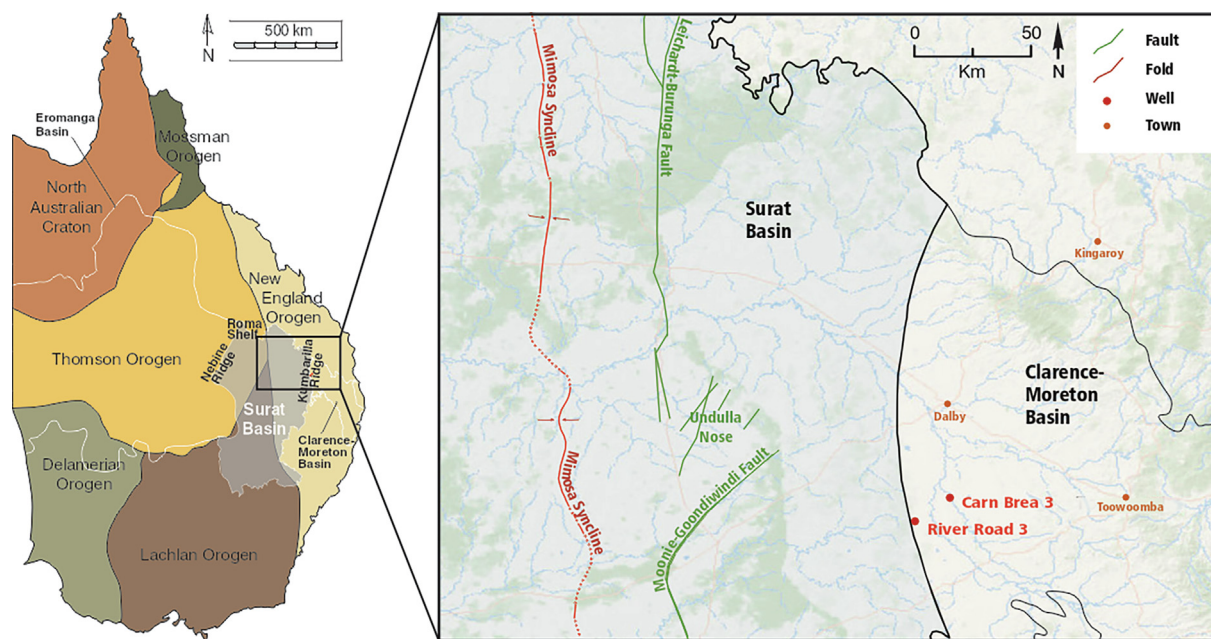


Fig. 2. Left: location of the Surat Basin in the context of the building blocks of the Tasmanides (modified after Sobczak et al., 2022). Right: outline of the north-eastern Surat Basin with relevant structural features, showing the location of the River Road 3 and Carn Brea 3 wells sampled in this study. Note that although the wells are located on the Clarence-Moreton side of the surface boundary between the two basins, the subsurface transition is gradual. The sedimentary profiles described in this paper show a clear affinity to the Walloon Coal Measures of the Surat Basin and have been classified as part of the Surat succession in previous studies (Shields & Esterle, 2016; Shields et al., 2017a).

fore, cannot be used as lithostratigraphic markers (Hamilton et al., 2014). However, they offer the unique opportunity to identify potential regional marker horizons through precise U-Pb CA-ID-TIMS dating of zircons contained in the tuffs.

The depositional environment of the Walloon Coal Measures has been widely interpreted as non-marine, low-energy alluvial plain with extensive deposition in peat mires and minor lacustrine sedimentation (Exon, 1976; Hamilton et al., 2014; Jones & Patrick, 1981; Ryan et al., 2012; Martin et al., 2013; Shields & Esterle, 2015; Shields et al., 2017a; 2017b; Wainman & McCabe., 2019; Yago & Fielding, 1996; Zhou et al., 2017). Morphology of the fluvial system varies spatially and temporally, showing characteristics of meandering, as well as anastomosing channels. The proportions of channel, overbank, swamp and lacustrine subenvironments also vary over short distances throughout the succession (Shields & Esterle, 2015; Zhou et al., 2017). The entirely non-marine character of the Walloon Coal Measures has been recently challenged based on sedimentological and palynological evidence (Wainman et al., 2018b; 2019; Wainman & McCabe., 2019). The abundance of dinoflagellate cysts, acritarchs, double mud drapes and lenticular bedding suggests marine influence on sedimentation, both in terms of tidal influence and brackish conditions.

3. Methods

3.1. Zircon dating

As tuffs contain syn-depositional primary zircons that are assumed to approximate the depositional ages of adjacent sedimentary units (e.g., Fedo et al., 2003; Gehrels, 2014), the sampling strategy for isotopic dating involved identifying tuff horizons preserved within coal and mudstone beds. Eleven tuff samples were collected from two wells: Carn Brea 3, and River Road 3, targeting the Walloon Coal Measures (Fig. 2). These wells were selected based on their proximity to seismic lines, comprehensive coverage of the Surat Basin stratigraphy, and the availability of core and wireline data.

Tuff horizons with visible medium to coarse sand-grade components and high Zr content (>250 ppm) were targeted. Zirconium content was assessed directly on the core, before sampling, using an Olympus Delta Handheld XRF Analyser. Several samples were collected from very close depth intervals for quality control. To ensure unbiased results, all samples were sent for analyses with only the sample numbers, which contained no location or stratigraphic information. Sample details are listed in Table 1.

Zircon dating was performed at the Boise State University Isotope Geology Laboratory (Idaho, USA). Standard techniques were used for mineral separation. Zircon grains were annealed at 900 °C for 60 h in a muffle furnace, mounted in epoxy resin and polished to expose the grain interiors. To select elongated, euhedral grains with simple oscillatory zoning, cathodoluminescence (CL) images were obtained with a JEOL JSM-300 scanning electron microscope and Gatan MiniCL (Fig. 3 and Appendix 1). Up to 50 zircon grains per sample were dated by Laser Ablation Inductively Coupled Plasma Mass Spectrometry (LA-ICP-MS) to help assess the probability of producing meaningful CA-ID-TIMS results. Selected trace elements were also analysed during the LA-ICP-MS analysis (see Appendix 1 for methodology and results). LA-ICPMS dating was performed using a ThermoElectron X-Series II quadrupole ICPMS and New Wave Research UP-213 Nd:YAG UV (213 nm) system. In-house analytical protocols, standard materials and data reduction software were used for acquisition and calibration of U-Pb dates (Appendix 1).

Zircon grains were selected for CA-ID-TIMS dating based on the homogenous SEM-CL response (Fig. 3), lack of inherited (older)

Table 1
A summary of CA-ID-TIMS U-Pb zircon geochronology results from the Walloon Coal Measures in Carn Brea 3 and River Road 3 samples.

Sample ID	Well	Depth (m)	Stratigraphic unit ¹	Weighted mean age (Ma)	95 % CI ² (Ma)	MSWD	Probability of fit	n	Total n	Other dates/comments
UQ-S10	Carn Brea 3	234.4–234.5	Juandah CM ² (Macalister Seam)	158.84	0.05	1.4	0.23	4	7	3 at 158.94–159.57 Ma This is a maximum depositional age. 6 others at 160.08–161.94 Ma are detrital/inherited
UQ-S11	Carn Brea 3	273.6–273.7	Juandah CM (Wambo Seam)	159.79	0.07			1	7	1 at 157.2 Ma (likely Pb loss), 1 at 160 Ma, 1 at 169 Ma (likely detrital/inherited)
UQ-S14	Carn Brea 3	273.8–273.9	Juandah CM (Wambo Seam)	159.91	0.04	1.1	0.36	7	10	1 at 162.93 Ma (likely Pb loss), 1 at 163.2 Ma (likely detrital/inherited)
UQ-S5	Carn Brea 3	491.0–491.3	Upper Taroom CM	163.00	0.05	2.1	0.10	4	8	1 at 174.6 Ma, 1 at 176.9 Ma
UQ-S17	Carn Brea 3	491.5–491.6	Upper Taroom CM	163.05	0.08	1.9	0.13	4	6	
UQ-S12	Carn Brea 3	554.0–554.1	Lower Taroom CM (Condamine Seam)	165.88	0.11	2.3	0.07	4	4	
UQ-S6	Carn Brea 3	554.2–554.3	Lower Taroom CM (Condamine Seam)	165.75	0.07	0.7	0.55	4	10	6 at 166.0–166.3 Ma (likely detrital/inherited)
UQ-S18	River Road 3	292.5–292.6	Juandah CM (Wambo Seam)	159.49	0.35	0.5	0.48	2	8	This is a maximum depositional age. 6 others at 159.6–160.2 Ma
UQ-S15	River Road 3	292.7–293.1	Juandah CM (Wambo Seam)	159.69	0.03	0.3	0.90	5	5	
UQ-S16	River Road 3	499.8–500.0	Upper Taroom CM	165.08	0.03	1.1	0.36	6	6	

¹ Nominal stratigraphic units are taken from the well completion reports.

² CM – Coal Measures.

³ CI – Confidence Interval based on the Student's t-distribution

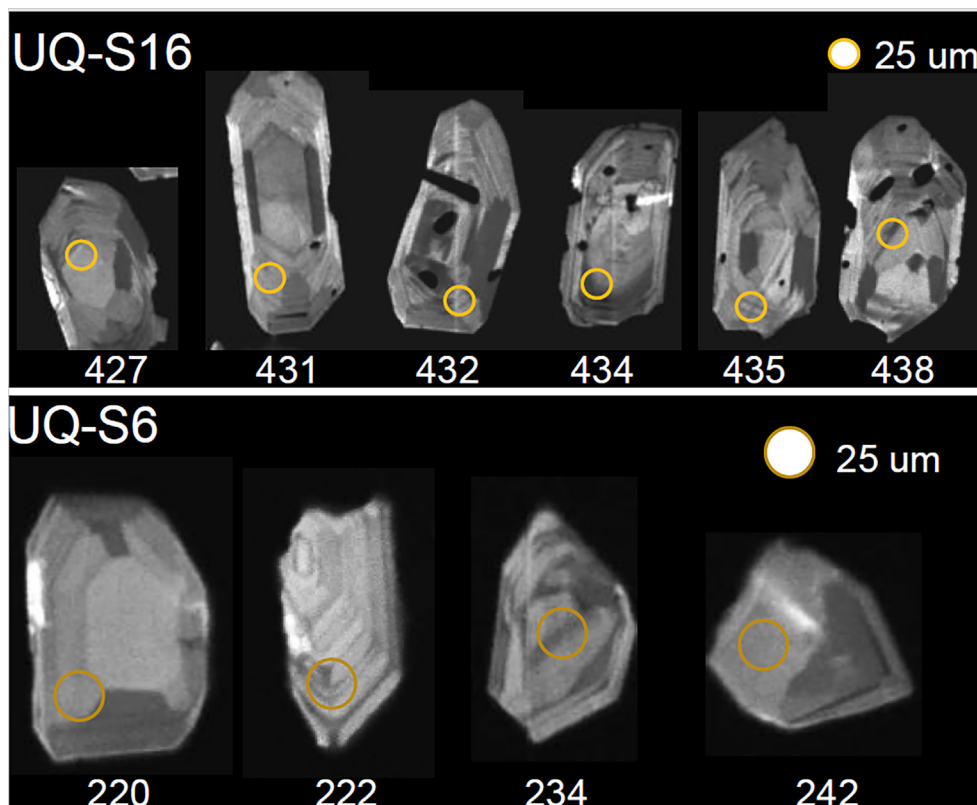


Fig. 3. Cathodoluminescence images of characteristic zircon grains from River Road 3 (top row) and Carn Brea 3 (bottom row) samples that were dated by CA-ID-TIMS and were included in weighted mean age interpretations.

cores, the elongate and sharply faceted grain morphology indicating primary volcanic origin (e.g., Corfu et al., 2003), and the lack of visible sedimentary reworking, and the results of the LA-ICP-MS dating. Selected zircon grains were removed from the epoxy mounts and subsequently dated by CA-ID-TIMS using methods modified after Mattinson (2005). Isotopic measurements were made on a GV Isoprobe-T multicollector thermal ionization mass spectrometer equipped with an ion-counting Daly detector. Weighted mean $^{206}\text{Pb}/^{238}\text{U}$ CA-ID-TIMS dates are calculated from statistically equivalent dates (probability of fit > 0.05). Errors on weighted mean dates are reported at 95 % confidence of a Student's t-distribution, and errors on single analyses are at 2σ . Detailed analytical procedures are described in Appendix 1.

Bayesian age stratigraphic models for the Carn 3 Brea and River Road 3 wells (Fig. 2) were made using stratigraphic positions, depositional U-Pb zircon weighted mean ages determined by CA-ID-TIMS, and the modified Bchron Bayesian age stratigraphic model in the R programming language (Trayler et al., 2019; R Core Team, 2023). Posterior ages for palynology horizons were interpreted from the medians of the posterior distributions with uncertainties corresponding to the 95 % highest density intervals (HDI) of the model runs.

3.2. Palynology

Nineteen samples were collected from fine-grained lithologies within the Walloon Coal Measures from the Carn Brea 3 and River Road 3 wells for palynological analysis (Fig. 2). Eleven samples were collected from Carn Brea 3 and eight samples were collected from River Road 3. Importantly, no stratigraphic information on the samples was provided to MGPaleo.

The samples were processed and analysed by MGPaleo (Malaga Laboratory, Perth). Standard palynological preparatory techniques, as outlined by Phipps and Playford (1984), Wood et al. (1996), and (Brown et al., 2008), were used. The samples were washed to remove modern spore-pollen contaminants and drilling additives and then crushed to a 2–5 mm diameter grit. The samples were then immersed in hydrochloric acid (32 %), to break down any calcareous minerals. The remaining mineral and organic residue was added to cold hydrofluoric acid (48 %) for 24 h to digest the siliciclastic minerals. The samples were then washed with hydrochloric acid to eliminate any fluorides that may have formed prior to heavy mineral separation using lithium heteropolytungstates (LST; specific gravity 2.1). The resulting float was neutralized before filtering through 10 μm and 100 μm nylon sieves to remove fine organic particles and coarse woody fragments. Kerogen slides were mounted using this unoxidized organic fraction, and the remaining kerogen fraction was oxidised (30 sec) in nitric acid (69 %) before mounting on glass slides for analysis. Samples counts were made with a target of approximately 200 palynomorphs. Subsequent species identified in the samples were simply recorded as present. The recorded palynomorph assemblages were then assigned to the palynostratigraphic zonation scheme of Price (1997).

This first pass stratigraphic-independent analyses of MGPaleo was then placed into stratigraphic context at the University of Queensland. Palynological data was recorded and plotted in the software package Stratabugs by both palynological groups. Photomicrographs (Fig. 6) were taken using an Olympus BX53 trinocular microscope and attached Olympus DP26 camera.

MGPaleo palaeoenvironmental assessments were based on the proportions of marine microplankton (saline algae) to

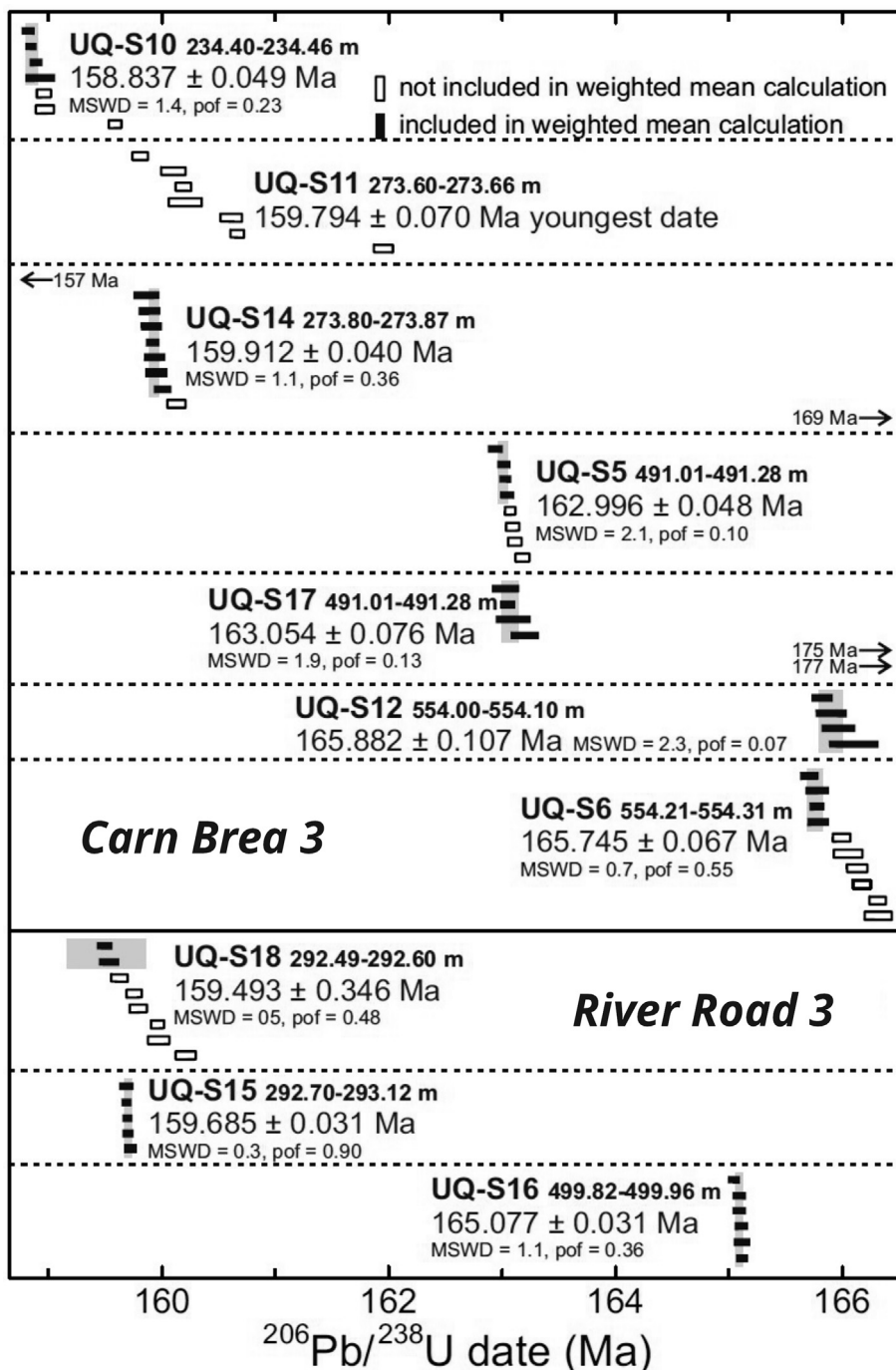


Fig. 4. Ranked date plot for the $^{206}\text{Pb}/^{238}\text{U}$ CA-ID-TIMS zircon ages with errors at the 95 % confidence interval for all samples from the River Road 3 and Carn Brea 3 wells. Plotted with Isoplot 3.0 (Ludwig, 2003). Weighted mean ages are represented by grey box behind the error bars. MSWD = Mean Square of Weighted Deviation; pof = probability of fit.

non-marine spores, pollen and freshwater algae, combined with an evaluation of marine microplankton diversity where applicable. Additional context was based on the inferred plant affinities of the recovered palynomorphs to help reconstruct the parent vegetation that produced the palynological assemblage. A table listing the affinities of the palynomorphs identified in this study is included in Appendix 2. These affinities are based largely on the annotated catalogue of Balme (1995) of in-situ spores and pollen grains.

4. Results

4.1. CA-ID-TIMS u-pb zircon geochronology

The isotopic age results from 11 samples that were dated by CA-ID-TIMS are summarised in Table 1 and Fig. 4. The results of Bayesian age stratigraphic modeling are shown in Fig. 5. Full results, including LA-ICP-MS analysis prior to CA-ID-TIMS, are available in Appendix 2.

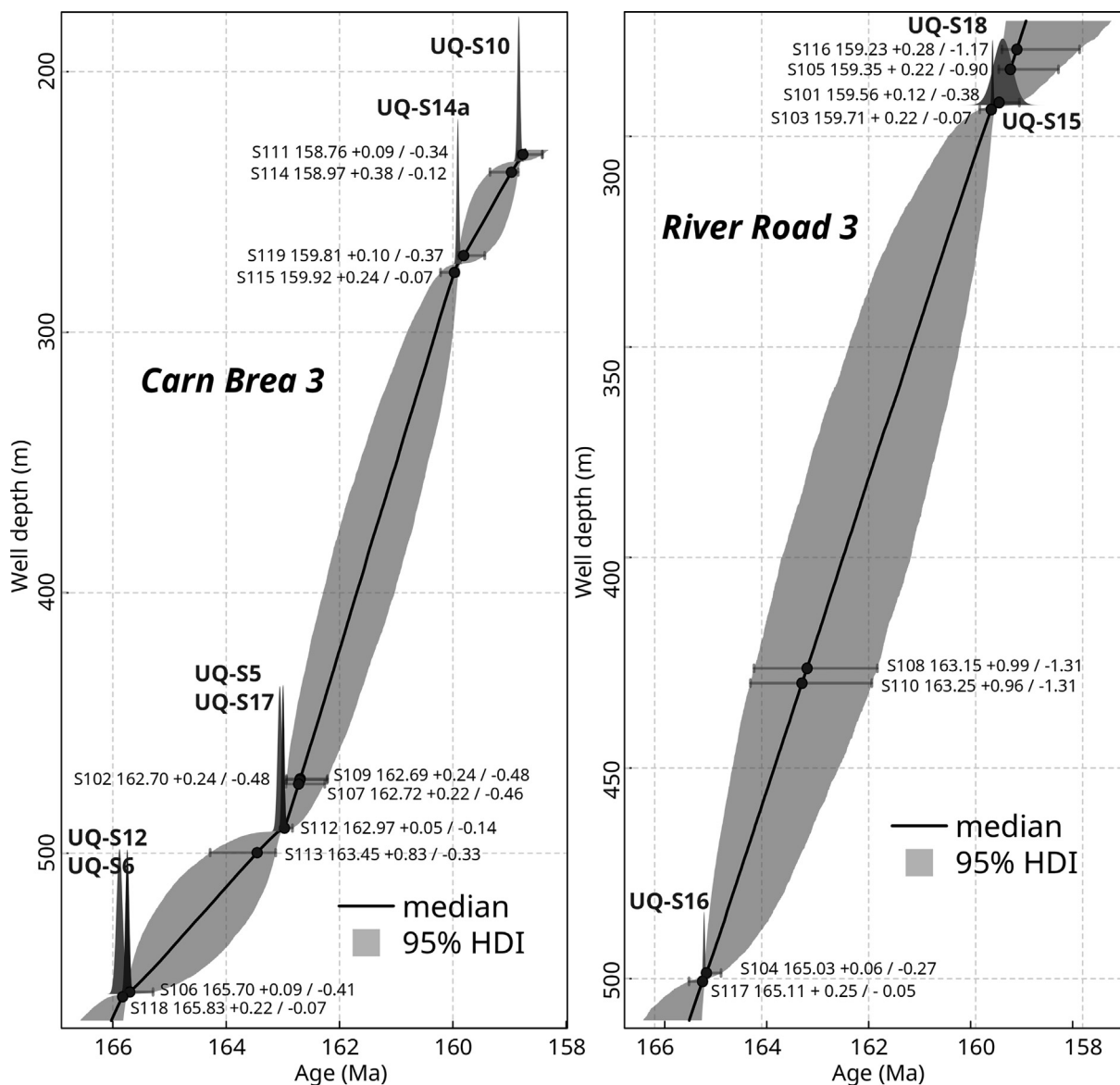


Fig. 5. Bayesian age stratigraphic models for the Carn Brea 3 and River Road 3 wells, using well depths as stratigraphic positions, depositional U-Pb zircon ages of tuffs determined by CA-ID-TIMS age likelihoods, and the modified Bchron Bayesian stratigraphic age model (Trayler et al., 2019). Posterior ages for palynology horizons that are indicated are derived from the median and 95% highest density intervals (HDI) of the modelling results. Palynology horizons are denoted by samples beginning with S and tuff samples are denoted by samples beginning with UQ.

Between 4 and 10 (average of 7) zircon grains per sample were analysed by CA-ID-TIMS. Depositional ages were interpreted from a weighted mean of statistically equivalent grains in each sample (range of 3 to 7). Several samples contained additional grains that are younger and older than the group upon which the weighted mean is based (Table 1 and Fig. 4). We interpret the younger dates (in samples UQ-S5, UQ-S11 and UQ-S14) to be biased by Pb loss and are therefore not interpreted as meaningful dates. It is also possible that the younger grains were incorporated as detritus from the well drilling process. The older grains (in samples UQ-S5, UQ-S6, UQ-S10, UQ-S11, UQ-S14, UQ-S17, and UQ-S18: Fig. 4) are interpreted as either detrital (in a reworked tuff) or inherited in the magma chamber and in either case, do not provide meaningful information on depositional ages.

Of the eight samples collected from Carn Brea 3, three samples were collected near other samples to determine quality assurance (Table 1). Sample UQ-S5 (163.00 ± 0.05 Ma) was collected directly above UQ-S17 (163.05 ± 0.08 Ma) and both samples yielded ages

that are statistically equivalent. UQ-S12 (165.88 ± 0.11 Ma), which is stratigraphically just above UQ-S6, is just outside error of UQ-S6 (165.75 ± 0.07 Ma). Similarly, UQ-S11 (159.79 ± 0.07 Ma), which was sampled closely above sample UQ-S14, is just outside error of UQ-S14 (159.91 ± 0.04 Ma). Unlike the rest of the ages, the final age from sample UQ-S11 is based on one grain only and is interpreted as a maximum depositional age, with some older grains in the sample (160.08–161.94 Ma) interpreted as detrital or inherited (Table 1; Appendix 2).

4.2. Palynology

The palynological assemblages recovered from the samples were of reasonable preservation and yielded sufficient identifiable palynomorphs to allow for assemblage counts of 240–281 to be carried out. Summary results are presented in Table 2 and selected species are shown in Fig. 6. The full counts for each sample are given in Appendix 2.

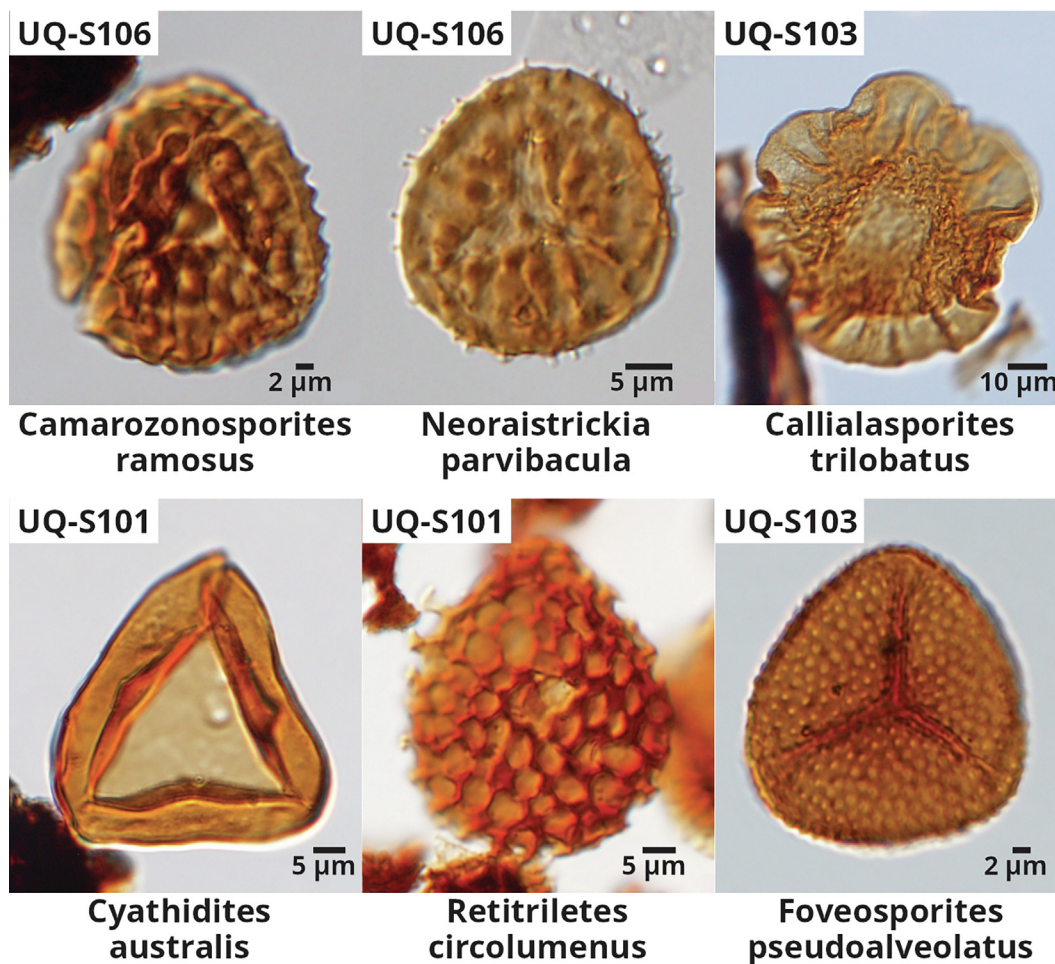


Fig. 6. Photomicrographs of selected key spore-pollen taxa from Carn Brea 3 (UQ-S106) and River Road 3 (UQ-S103 and UQ-S101).

Of the 11 samples from Carn Brea 3, six samples produced a high microfossil yield. These samples were dominated by spore-pollen and contained high to very high species diversity (Table 2). Three samples produced a moderate microfossil yield, which was also dominated by spore-pollen, with contained moderate to high species diversity. One sample (S102), however, produced a low microfossil yield. While the microfossils were still dominated by moderately diverse spore-pollen, sample S102 did contain the highest percentage of algal palynomorphs.

Of the eight samples from River Road 3, six have a high microfossil yield and two have a moderate microfossil yield. All eight samples are dominated by spore-pollen, and their species diversity is high to very high. In contrast to the Carn Brea 3 assemblages, in which no acritarchs were identified, three of the assemblages from River Road 3 contained trace amounts of spinose acritarchs.

Using the Price (1997) alphanumeric zonation, combined with information from the work of McKellar (1998) on the Roma Shelf, Table 2 gives the assigned palynostratigraphic zones based on the identification of index fossils within each sample. Fig. 8 shows the samples in stratigraphic order with assigned zonations based on that, as well as the stratigraphic relationship of the palynological and geochronological samples. On this basis, palynologically, all samples fall within the range of APJ4.2 to APJ4.3. Specifically, all Carn Brea 3 samples from 555.15 to 231.81 m fall within APJ4.2 (Fig. 8). Whereas the River Road 3 samples from depths of 500.7 to 426.26 m belong to APJ4.2. Samples S103 and S101 (293.69 to 291.89 m) fall between APJ4.2 and APJ4.3. The top two samples, 284.12 to 279.29 m fall within APJ4.3 (Fig. 8).

The palynological assemblages of both wells were dominated by contemporaneous pollen and spores. Reworked Permian palynomorphs were present in trace amounts in some, but not all samples. Of the non-spore pollen palynomorphs, the most abundant were those of green algal origin, primarily *Botryococcus* and *Leiosphaeridia*. These algal palynomorphs mostly form only a minor component of each assemblage, except for sample S102, where *Leiosphaeridia* form 17 % of the total assemblage. The palynological assemblages of the two wells show little or no evidence of marine influence with no dinoflagellates recognised in either well, and spinose acritarchs being absent from the sampled interval of Carn Brea 3, and only present as a trace component of three of the River Road 3 samples.

Overall, palynomorphs produced by conifers are the most abundant, followed by those produced by ferns, lycophytes, bryophytes and seed ferns (Fig. 7). The relative abundance of the seed ferns is likely to be under-represented in this data as all bisaccate pollen in the sample counts was recorded under 'bisaccates undifferentiated' and have all been assigned to the conifers here as the most commonly observed bisaccate pollen were *Podocarpidites*. As a result, only the pollen of *Vitreisporites* is recognised as being of clear seed fern origin. The two most abundant forms of conifer derived pollen in these samples were *Araucariacites* and *Callialasporites* (Araucariaceae) and 'bisaccate undifferentiated' (dominated by Podocarpaceae), except in sample S118, where *Perinopollenites elatoides* (Taxodiaceae) comprises 68 % of the total assemblage. On this basis, the two excursions in the relative abundance of conifer pollen observed in the lowermost samples of both wells (Fig. 7)

Table 2
Palynology results and posterior ages from Bayesian modeling. CM – Coal Measures. CB3 – Carn Brea 3. RR3 – River Road 3.

Sample ID	Well	Depth (m)	Nominal unit ¹	Micro-fossil yield	Percentage (%)							Zone	Environ-ment ³	Key datums	Posterior ages ± 95 % credible intervals (Ma) ⁴		
					Microplankton			Spore-pollen							Age	+	–
					Dino flag.	Spiny ac.	Other	Diversity	Spore-pollen ²								
S111	CB3	231.81–231.84	Juandah CM (Macalister Seam)	High	0	0	4	98	High	APJ3.3.1/A. fissus	Non-marine	<i>K. lacunus</i> , <i>S. manifestus</i> , <i>A. saevus</i>	158.76	0.09	0.34		
S114	CB3	238.55–238.67	Juandah CM (Macalister Seam)	High	0	0	1	99	High	APJ3.3.2/C. ramosus	Non-marine	<i>C. ramosus</i> , <i>S. manifestus</i>	158.97	0.38	0.12		
S119	CB3	270.57–270.7	Juandah CM (Wambo Seam)	Mod. low	0	0	0	100	High	APJ3.3.1/A. fissus	Non-marine	<i>S. manifestus</i> , <i>C. dampieri</i> , <i>K. lacunus</i>	159.81	0.10	0.37		
S115	CB3	277.04–277.18	Juandah CM (Wambo Seam)	High	0	0	0	100	High	APJ3.3.2/C. ramosus	Non-marine	<i>C. ramosus</i>	159.97	0.24	0.07		
S109	CB3	471.38–471.48	Upper Taroom CM	Mod.	0	0	5	95	Mod.	No older than APJ3.1/C. torosa	Non-marine	Degraded Kerogen. No markers found	162.69	0.24	0.48		
S102	CB3	471.85–471.97	Upper Taroom CM	Low	0	0	17	83	Mod.	APJ3.2/A. fissus	Non-marine	<i>C. dampieri</i> , <i>S. manifestus</i> . Frequent <i>Leiospheres</i> and <i>Botryococcus algae</i>	162.70	0.24	0.48		
S107	CB3	473.38–473.47	Upper Taroom CM	High	0	0	2	98	High	APJ3.3.1/A. fissus	Non-marine	<i>K. lacunus</i> , <i>S. manifestus</i>	162.72	0.22	0.46		
S112	CB3	490.25–490.4	Upper Taroom CM	High	0	0	1	99	V. high	APJ4.2.1/R. circoluminus	Non-marine	<i>C. ramosus</i> , <i>S. manifestus</i> , <i>P. whitfordensis</i>	162.97	0.05	0.14		
S113	CB3	499.69–499.83	Upper Taroom CM	High	0	0	0	100	High	APJ4.2.1/R. circoluminus	Non-marine	<i>A. saevus</i> , <i>P. whitfordensis</i>	163.45	0.83	0.33		
S106	CB3	553.17–553.3	Lower Taroom CM (Condamine Seam)	Mod. low	0	0	1	99	High	APJ4.2.1/R. circoluminus	Non-marine	<i>P. whitfordensis</i>	165.70	0.09	0.41		
S118	CB3	555.0–555.15	Lower Taroom CM (Condamine Seam)	Mod. high	0	0	2	98	Mod.	APJ4.2.1/R. circoluminus	Non-marine	<i>P. whitfordensis</i> , Superabundant <i>P. elatoides</i>	165.83	0.22	0.07		
S116	RR3	279.29–279.38	Juandah CM (Wambo Seam)	High	0	0	6	94	High	APJ4.2.1/R. circoluminus	Non-marine	<i>P. whitfordensis</i> , <i>S. manifestus</i> , frequent <i>Botryococcus algae</i>	159.23	0.28	1.17		
S105	RR3	284.02–284.12	Juandah CM (Wambo Seam)	High	0	0	1	99	V. high	APJ4.3/C. glebulenuts	Non-marine	<i>C. glebulentus</i> , <i>P. whitfordensis</i>	159.35	0.22	0.90		
S101	RR3	291.89–292.0	Juandah CM (Wambo Seam)	Mod.	0	<1	0	100	V. high	Likely APJ4.3/C. glebulentus	Brackish	<i>C. burgeri</i> , <i>C. ramosus</i> , <i>S. manifestus</i> , <i>Micrhystridium</i> spp.	159.56	0.12	0.38		
S103	RR3	293.53–293.69	Juandah CM (Wambo Seam)	Mod.	0	0	2	98	V. high	APJ3.3.2/C. ramosus	Non-marine	<i>C. ramosus</i> , <i>S. manifestus</i>	159.71	0.22	0.07		
S108	RR3	426.26–426.33	Upper Taroom CM	High	0	<1	2	98	High	APJ4.2.1/R. circoluminus	Brackish	<i>C. ramosus</i> , <i>P. whitfordensis</i> , <i>Micrhystridium</i> spp.	163.15	0.99	1.31		
S110	RR3	429.77–429.87	Upper Taroom CM	High	0	0	1	99	High	APJ3.3.2/A. fissus	Non-marine	<i>A. saevus</i> , <i>K. lacunus</i> , <i>C. ramosus</i>	163.25	0.96	1.31		
S104	RR3	498.6–498.68	Upper Taroom CM	High	0	0	3	97	V. high	APJ4.2.2/A. norrisi	Non-marine	<i>C. ramosus</i> , <i>A. norrisi</i> , <i>R. circoluminus</i> , <i>C. perforata</i>	165.03	0.06	0.27		
S117	RR3	500.59–500.7	Upper Taroom CM	High	0	<1	3	97	High	Likely APJ4.2/R. circoluminus	Brackish	<i>S. asperata</i> , <i>K. lacunus</i> , <i>A. saevus</i> , <i>C. ramosus</i> , <i>Micrhystridium</i> spp.	165.11	0.25	0.05		

¹ Units taken from the Well Completion Reports.

² Diversity: Very high (30 + species); High (20–29 species); Moderate (10–19 species); Low (5–9 species); Very low (1–4 species).

³ Environment is based on the percentage of Dinoflagellate. Where Dinoflagellate are absent, the presence or absence of Spiny Acritarchs differentiates Brackish versus non-marine environments.

⁴ Calculated from the median and 95% highest density interval of the age models in Fig. 5, constructed using the modified Bchron Bayesian age model (Trayler et al., (2019)).

appear to be unrelated as the spike in S117 is produced by the high numbers of 'undifferentiated bisaccates', primarily of the *Podocarpaceae* type. Of the spores, the numerically most dominant members of the assemblages are *Cyathidites* (Matoniaceae), *Osmundacidites* (Osmundaceae) and *Retitriletes* (Lycopodiophyta).

4.3. Trace elements

The trace elements were analysed for all zircon crystals dated via CA-ID-TIMS and full results are provided in Appendix 1. Trace elements that formed part of the weighted-mean age were from

zircons that were interpreted as syn-depositional rather than reworked or detrital. The zircons from Carn Brea 3 range in Ti from 3.27 to 14.31 ppm (average 6.59 ppm) and the zircons from River Road 3 range from 3.03 to 17.21 ppm (average 8.75 ppm). The Ta concentration in Carn Brea 3 is predominantly less than 0.7 ppm, except in one sample that is 1.04 ppm, the Nb is variable but always less than 3 ppm, and the Y concentration is predominantly less than 3000 ppm (Fig. 9). In the River Road 3 zircons, all except two of the Juandah Coal Measures samples have Ta concentrations greater than 1.0 ppm, the Nb is overall less than 4 ppm and the Y is generally below 2200 ppm. Both Nb and Y concentrations in the

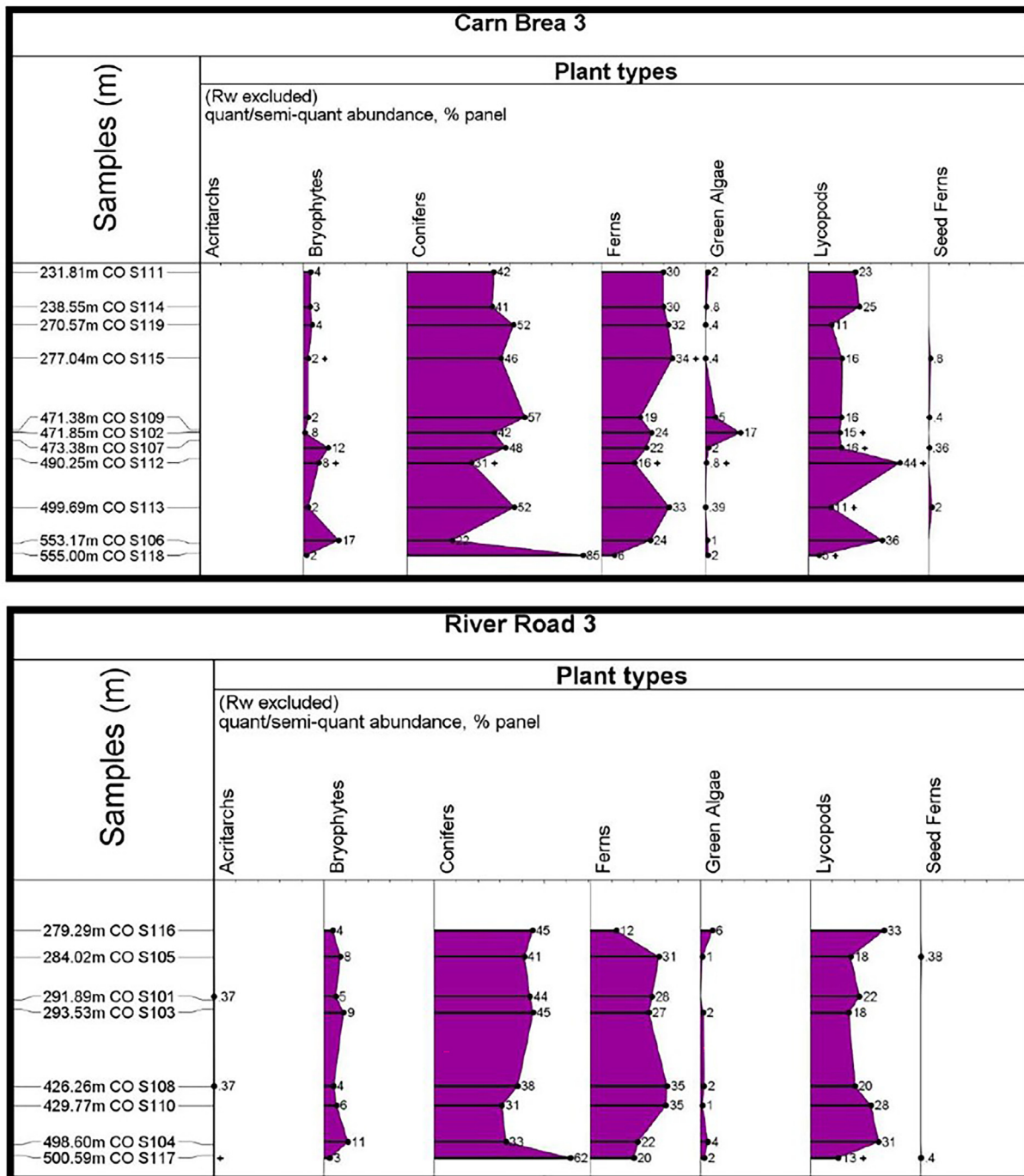


Fig. 7. Percentage compositions of in situ palynomorphs from the major plant groups in the River Road 3 and Carn Brea 3 samples. Not to scale. 'Bisaccates undifferentiated' have been included in the conifers rather than attempting to split out those members of the group produced by the seed ferns.

River Road 3 samples are generally higher for the Juandah Coal Measures than the Taroom Coal Measures.

5. Discussion

5.1. Radioisotopic ages

The first precise CA-ID-TIMS U-Pb zircon ages from tuff horizons in the Walloon Coal Measures from the eastern part of the basin were reported by Wainman et al., (2015; 2018b). The ages range from 162.54 ± 0.05 to 158.86 ± 0.04 Ma, placing the Walloon Coal Measures in the Upper Jurassic (Callovian to Oxfordian: Wainman et al., 2015). These results were significantly younger than previous age estimations based on palynoflora alone (Fig. 2; e.g., Cook et al., 2013). The age range of the Walloon Coal Measures was extended to 164.74 ± 0.04 and 149.78 ± 0.06 Ma based on a larger study of the tuff samples from across the Surat Basin (Wainman et al., 2018b).

The precise CA-ID-TIMS U-Pb zircon ages from tuff samples reported here are only the third set of isotopic ages reported from the Walloon Coal Measures to date. These new ages range from

165.88 ± 0.11 Ma to 158.84 ± 0.05 Ma. At a broad scale, the new precise U-Pb zircon ages do match with the existing data from nearby boreholes such as Stratheden 60, Stratheden 4, and Turalin 1 from Wainman et al., (2015; 2018b).

The lower part of the Walloon Coal Measures, the Taroom Coal Measures, sampled in the Carn Brea 3 and River Road 3 wells, range in age from 165.88 ± 0.11 to 163.05 ± 0.08 Ma. This age data range places the Taroom Coal Measures within the Callovian to lower-most Oxfordian (Figs. 10 and 11). Whereas, the Juandah Coal Measures, sampled from the Carn Brea 3 well, range from 159.91 ± 0.04 to 158.84 ± 0.05 Ma (Fig. 10), locating the Juandah Coal measures within the Oxfordian (Fig. 11). The 3.14 Ma age difference between the top sample from the Taroom and the lowermost sample from the Juandah Coal Measures likely reflects normal depositional rates over a ~ 200 m interval. However, rate of sedimentation over this period was probably variable, given that the Tangalooma Sandstone unit in between has reduced coal and is associated with the maximum flooding surface (Shields et al., 2017a), likely resulting in much slower deposition.

Based on our results and those of Wainman et al., (2015; 2018a; 2018b), it is clear that in the area of the Kumberilla Ridge, the age

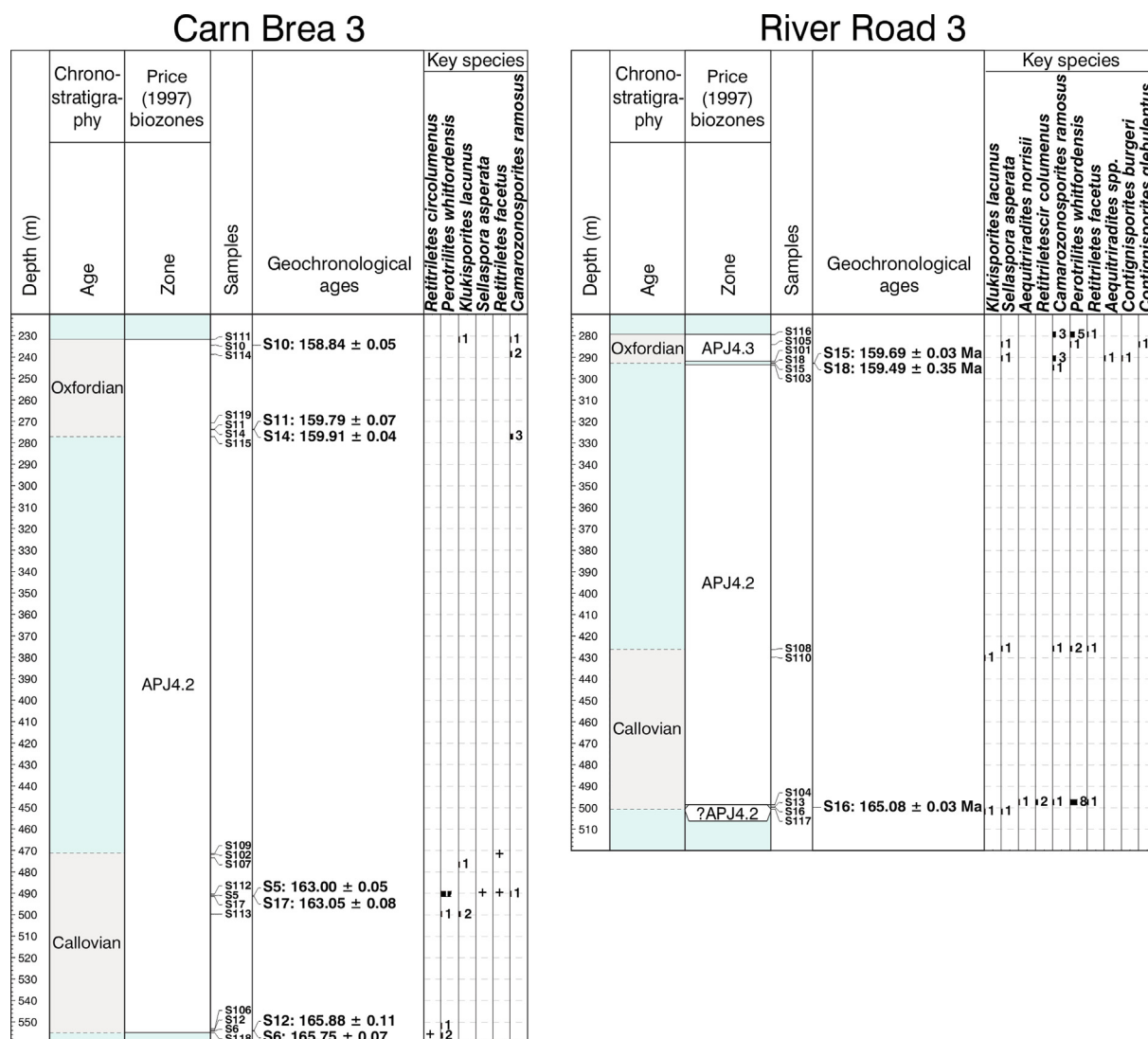


Fig. 8. Stratigraphic section of Carn Brea 3 and River Road 3 showing the palynozones with the CA-ID-TIMS ages. The key species column indicates in which samples palynomorphs of biostratigraphic significance were identified, and how many were recorded from each sample.

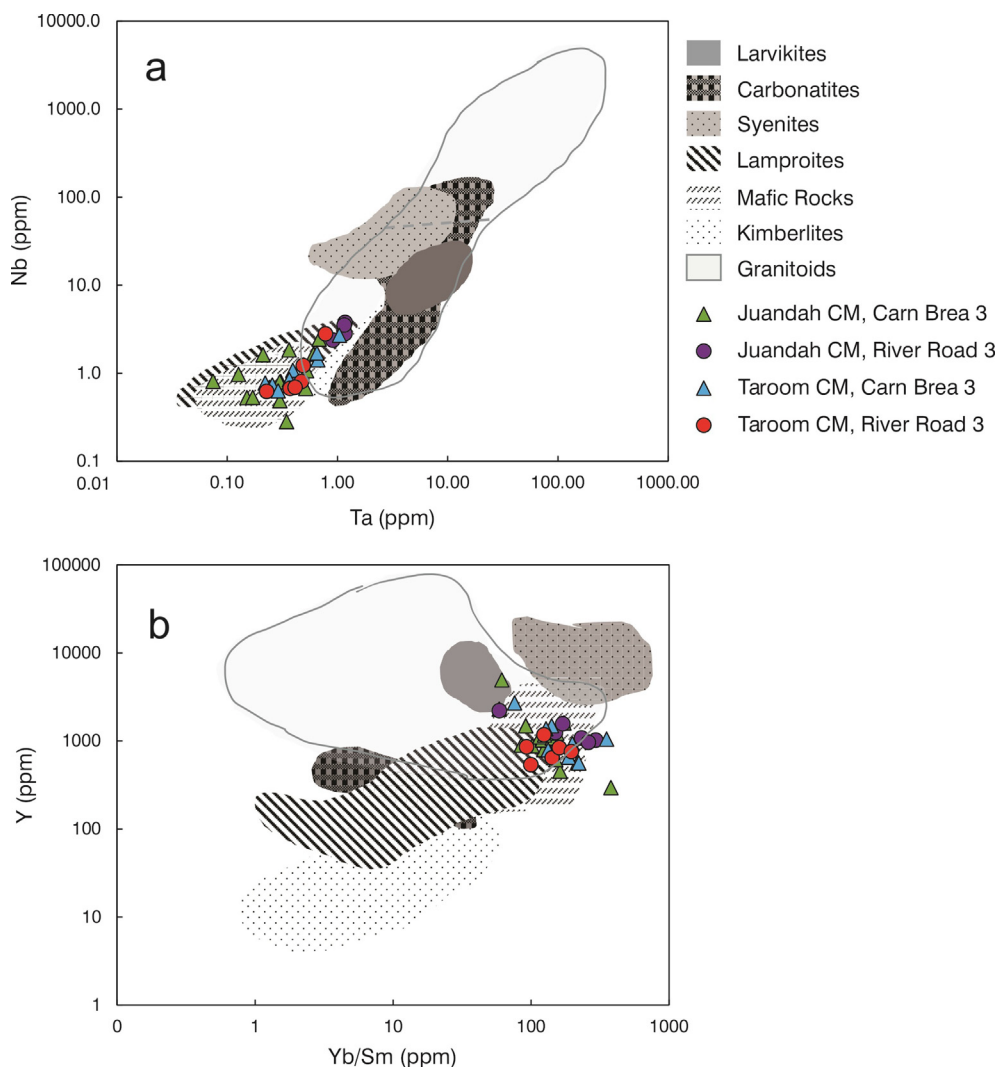


Fig. 9. Discrimination diagrams for zircon compositions, a) Nb vs Ta and b) Y vs Yb/Sm, shows where the *syn*-depositional zircons data plot against specific igneous rock types (data after Belousova et al. (2002) and reference therein). CM – Coal Measures.

of the Walloon Coal Measures should be considered Callovian to Oxfordian, rather than Aalenian–Callovian as per earlier studies (Exon and Burger, 1981; Jell, 2013; McKellar, 1998; Price, 1997).

Using chronostratigraphic markers can help provide an insight into the temporal evolution of the Walloon Coal Measures in different areas of the Surat Basin. In the east, at the Carn Brea 3 well, we observed that the Walloon Coal Measures formed over at least 7.5 Ma (28 m above the base of the Walloon Coal Measures to 32 m below the formation top, as per well completion report; Figs. 8 and 10). In the eastern-central part of the basin (Alderley 1 well), the Walloon Coal Measures were reported to have formed over at least a 4.5 Ma period, whereas, in the central-western part of the basin (Pleasant Hills 25 well), the 233 m-thick Walloon Coal Measures were reported to have formed over an 11 Ma period. In this area, Wainman et al., (2018b) inferred an unconformity within the Walloon Coal Measures, which does not extend to the eastern part of the basin. One of the uncertainties in locating this unconformity within the succession is that the nominal formation tops were taken unrevised from well completion reports and are not based on a consistent stratigraphic definition for the Walloon Coal Measures. Furthermore, Wainman et al.'s (2018b) interpretation is not necessarily supported by regional seismic and that may need further investigation. The new U–Pb ages reported here in conjunction with previously published maximum depositional ages and

CA-ID-TIMS ages (Andrade et al., 2023; in review), confirm no apparent unconformity in the Walloon Coal Measures in eastern part of the basin.

5.2. Biozones

Prior to precise isotopic dating, the age of the Walloon Coal Measures was estimated based on the palynological assemblages recovered with those from basins in New Zealand and on the north-west shelf of Australia (Fig. 1). In those locations, terrestrial palynomorphs have been recovered from near-shore marine deposits that are more readily linked to the international geological time scale. According to McKellar (1998) and Price (1997), the lower parts of the Walloon Coal Measures of the Surat Basin correlated with either the upper part of APJ4.2 or with APJ4.3, the middle part of the formation with APJ4.3 and the upper part of the formation with the lower parts of APJ5 (Fig. 1). It should be noted, however, that the majority of Surat Basin wells sampled for those studies came from the Roma Shelf region (Fig. 2) and surrounds. Furthermore, no palynological studies from the Surat Basin published to date have linked the vegetation communities to the sedimentological processes, so any lateral heterogeneity might be a function of variations in sedimentary environments and subsidence across the basin.

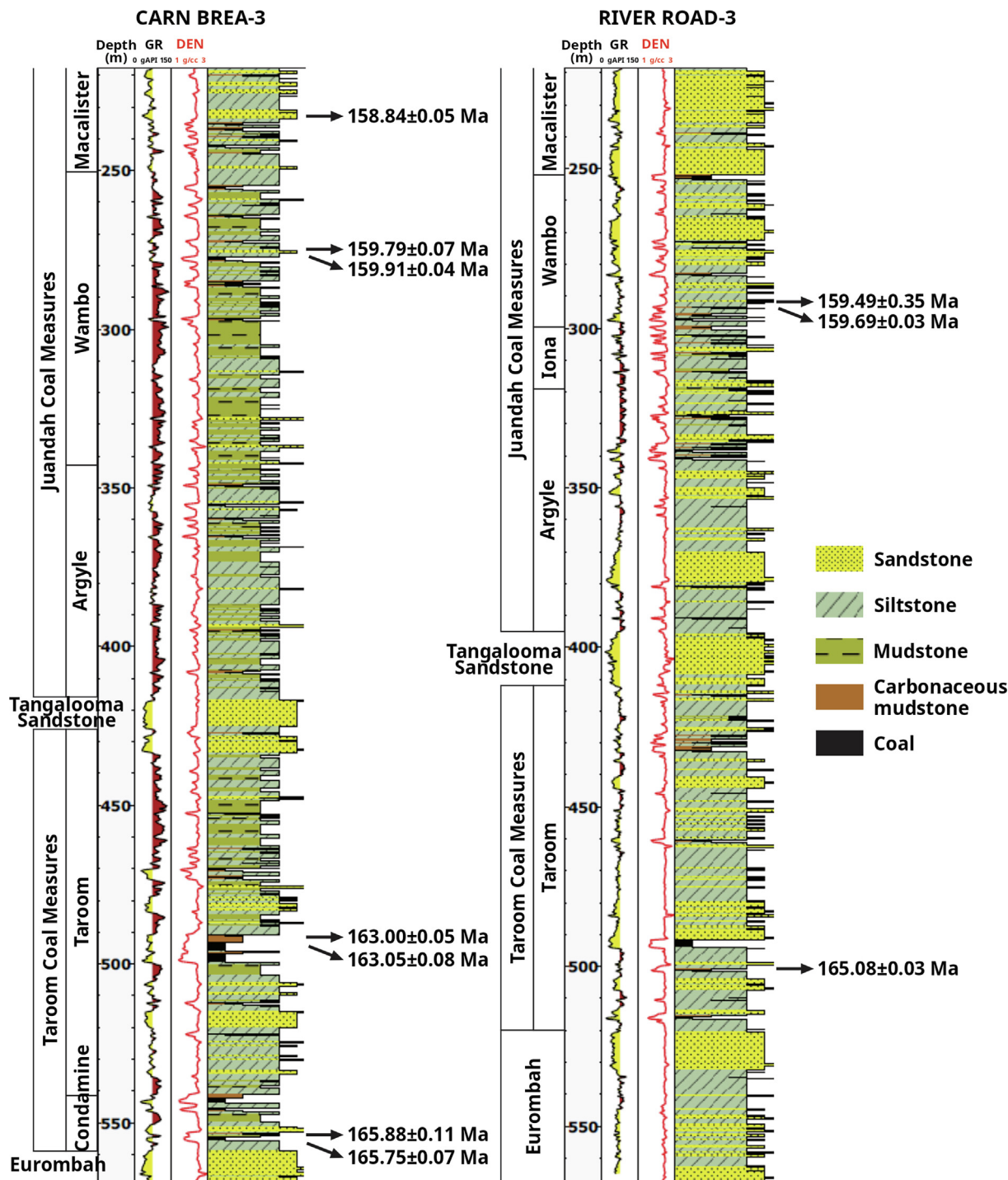


Fig. 10. Lithostratigraphic logs of Carn Brea 3 and River Road 3 with gamma-ray (GR) and density (DEN) logs, as well as the corresponding new CA-ID-TIMS zircon ages. Logs were plotted using Techlog software (Schlumberger).

The data from samples of the Carn Brea 3 well, correlate with APJ4.2 (Fig. 8). These include data from samples located stratigraphically in both the lower and upper part of the Walloon Coal Measures (Fig. 8 and Table 2). From the River Road 3 well, most sample data correlate with APJ4.2, excluding some of the younger data, which correlate with APJ4.3 (Fig. 8b). The youngest isotopic age, 158.07 ± 0.05 Ma, generally correlates with the stratigraphic zones of APJ4.2 to APJ4.3 (Fig. 11). This is significantly different to what Wainman et al., (2018a) observed in the central-western part of the basin, where at 158 Ma the stratigraphic zone is the younger APJ5. However, the presence of *Contignisporites* in samples

from the top of River Road 3, suggests some caution is appropriate with the lack of the younger palynozones in Carn Brea 3 and River Road 3 wells (Fig. 8). Comments made in Martin et al. (2013) and Wainman et al., (2018a) suggest that the parent plants that produced *Contignisporites* were more commonly found in the western part of the Great Australian Basin than the east, possibly due to habitat or climatic preferences. The distribution of *Murospora florida* has also been suggested to be partially environmentally controlled, and prone to occurring only sporadically in the lower part of its temporal range (McKellar, 1998). Wainman et al., (2018a) recorded an occurrence of *M. florida* from below a sample

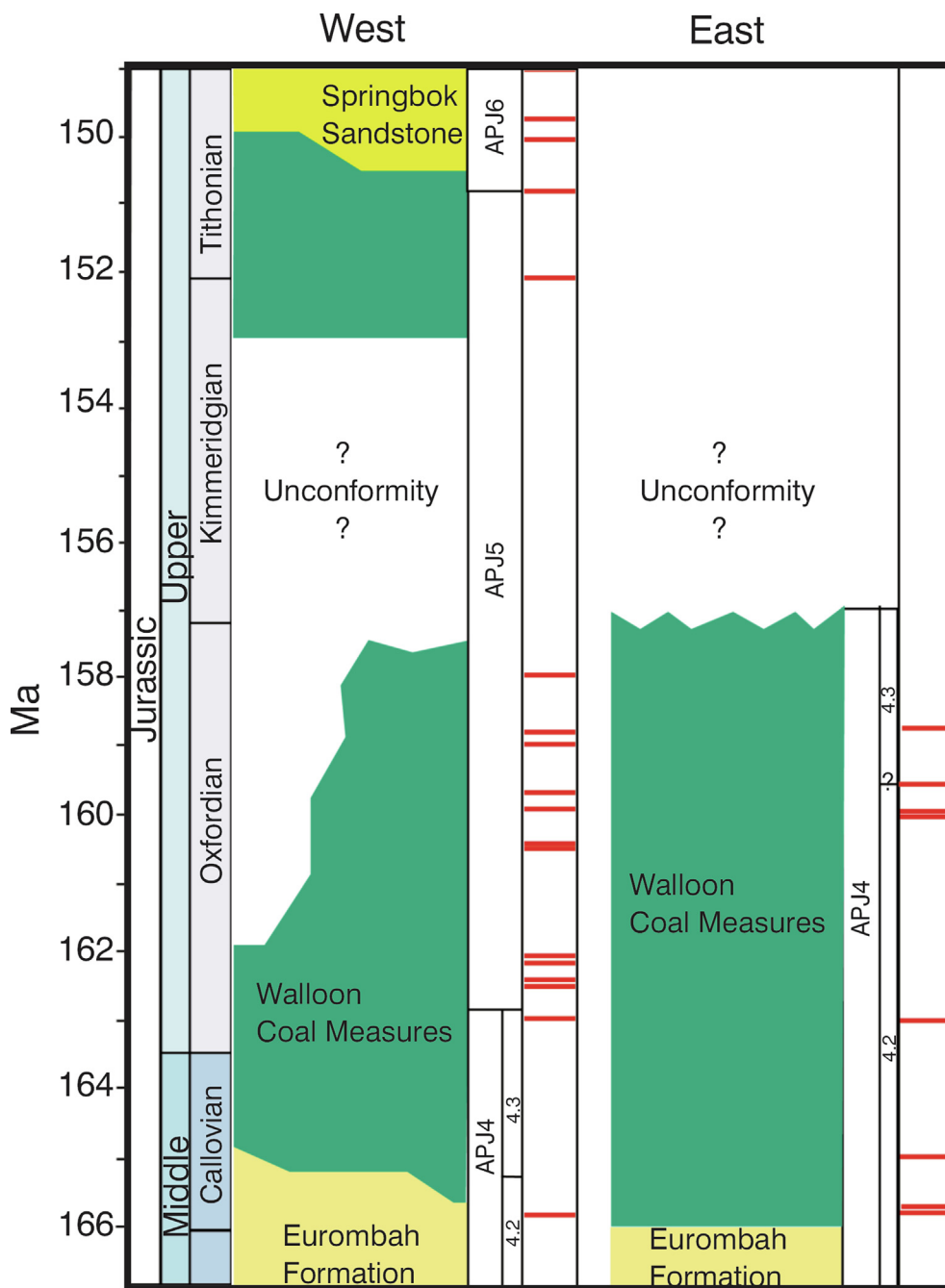


Fig. 11. Stratigraphy of the Walloon Coal Measures in the central-western vs eastern part of the Surat Basin showing associated palynozones from Carn Brea and River Road 3, as well as stratigraphic locations of existing CA-ID-TIMS ages (red lines). Modified after [Wainman et al., \(2018b\)](#). (For interpretation of the references to colour in this figure legend, the reader is referred to the web version of this article.)

isotopically dated as 162.54 ± 0.12 Ma in the nearby well Stratleden 4 (Fig. 2). Additional work with tighter sampling in the interval of APJ4.3 and basal APJ5 is needed to determine if these units are impacted by very sporadic appearances of their index fossils in the lower parts of these zones, or if the units are actually slightly diachronous between the east and west of the basin.

The Carn Brea 3 and River Road 3 boreholes are located in the eastern region of the Kumberilla Ridge, very close to the boundary of the Surat and Clarence-Moreton basins (Fig. 2). In the few studies reported from the Clarence-Moreton Basin, no species associated with zones APJ4.3 or APJ5 have been reported from the

Walloon Coal Measures (de Jersey, 1959; 1960; McKellar, 1978). As such, a finding that the majority of Walloon Coal Measures samples from Carn Brea 3 and River Road 3 wells at the boundary of the Surat and Clarence-Moreton basins largely belong to zone APJ4.2 is not unreasonable. These differences between the two basins have previously been interpreted as indicating that the Walloon Coal Measures are diachronous (Wainman et al., 2018a). The deposition of the formation began and ended earlier in the Clarence-Moreton Basin and eastern Surat Basin than in the western Surat Basin (Wainman et al., 2018a). Our data from the easternmost part of the basin are consistent with that interpretation.

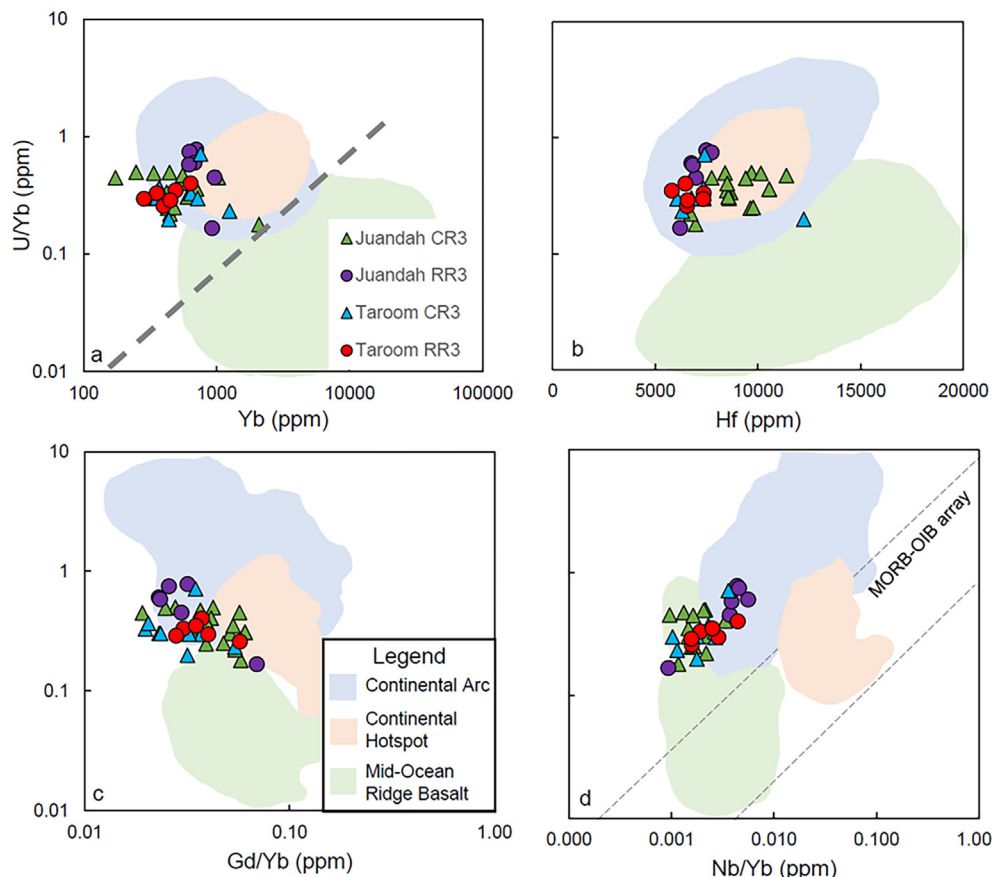


Fig. 12. Discrimination diagrams of a) U/Yb vs Nb/Yb; b) U/Yb vs Gd/Yb; c) U/Yb vs Yb; and d) U/Yb vs Hf, showing whether the new syn-depositional zircon data plots against general fields of MORB, Continental Arc and Continental hotspot (fields are after Grimes et al. (2007) and Carey et al. (2014)).

5.3. Palaeoenvironment

The new palynology results show that, with the exception of the spinose acritarch *Micrhystridium*, typically associated with brackish rather than fully marine conditions, all the in-situ palynomorphs observed in these samples were produced by terrestrial or freshwater plants. As *Micrhystridium* only occurs in trace amounts (<1%) in three of the River Road 3 samples, and is absent from the Carn Brea 3 samples (Fig. 8), a predominantly freshwater depositional environment is inferred, with variability associated with shifting floodplains and channels through time. The extremely low relative abundance of spinose acritarchs in River Road 3 combined with their absence from the Carn Brea 3 assemblages does suggest that Carn Brea 3 was located further from any marine influences than River Road 3, which is consistent with seismic interpretations of Shields et al., (2017a).

Green algae can grow in water bodies of any size, from small puddles through to streams and large lakes. The relatively low abundance of palynomorphs produced by this group in these samples is more characteristic of deposition in a fluvial, non-lacustrine setting (Fig. 8). The higher proportion of algal palynomorphs in sample S102 at Carn Brea 3 compared to the other samples is more suggestive of deposition in an environment with some standing water. Our interpretation of a fresh-water fluvial depositional environment, with areas of stagnant water is consistent with previous interpretations (Exon, 1976; Hamilton et al., 2014; Jones & Patrick, 1981; Martin et al., 2013; Shields & Esterle, 2015; Ryan et al., 2012; Shields et al., 2017a; 2017b; Wainman & McCabe., 2019; Yago & Fielding, 1996; Zhou et al., 2017).

Previous studies of the Walloon Coal Measures have suggested that the climate at the time of deposition was humid and temperate to warm (Hentschel et al., 2016; Hentschel, 2018; Martin et al., 2013; McKellar, 1998; Wainman et al., 2015). The palynological assemblages presented here are compatible with this interpretation. The relatively great abundances of palynomorphs produced by ferns, lycopods and bryophytes, as well as the presence of coal, strongly suggests plants growing in an environment where water abundance was not a limiting growth factor. Neither micro- nor megathermal climate is likely based on the sparsity of Jurassic species characteristic of either climate type in any of the sample assemblages. While it is difficult to determine what palaeotemperatures different families of plants preferred in the Mesozoic, these assemblages do seem to contain slightly more spores and pollen reminiscent of warmer rather than cooler conditions, notably including *Araucariacites* and *Classopollis* pollen, produced by the Araucariacean and Cheirolepidacean conifers (Abbink, 1998).

5.4. Volcanic origin

Zircons have specific trace element signatures, which allows us to identify what rock types zircons contained in tuff were originally formed in (e.g., Belousova et al., 2002; Gimes et al., 2015). Discrimination diagrams of U vs. Y and Y vs. Yb/Sm from Belousova et al. (2002), place the zircons from the tuff samples in this study in the mafic magmas field (Fig. 9). However, given the zircon morphology and low Th/U concentrations (Appendix 1), as well as the fact that zircons derived from mafic magmas are rare, the sample position on the discrimination diagrams is

interpreted as non-felsic, but intermediate rather than mafic. The predominantly low Ti, Ta, and Nb values lend support to a non-felsic magma origin (Belousova et al., 2002).

Discrimination diagrams based on zircon geochemistry can also be used to determine the tectonic setting that these zircons were formed in (Carey et al., 2014; Grimes et al., 2015). The trace element data from the Carn Brea 3 and River Road 3 wells plot on the continental arc to continental hotspot fields (Fig. 12). However, Fig. 12d shows that the new data plot outside the Mid-Ocean Ridge Basalt – Ocean Island Basalt array, on the continental arc zone. This suggests that the *syn*-depositional zircons dated by CA-ID-TIMS were derived from a continental arc, supporting Wainman et al.'s (2019) conclusion that the tuffs of the Walloon Coal Measures originated from a volcanic arc setting. The thin and discontinuous nature of the tuff beds is consistent with an extra-basinal origin. Previously reported increase in volcanic lithics in sandstone compositions from west to east additionally suggests an eastern, extra-basinal source (Bein, 2016). Some previous studies (e.g., Bryan et al., 1997; 2000; 2012; Cook et al., 2013; Wainman et al., 2019; Cooling et al., 2020) have suggested volcanic provinces on the active continental margin to the east such as the Whitsunday Province as potential sources of tuffs in eastern Australian basins. While the well-studied Whitsunday Province was not formed till after the deposition in the Surat Basin, it is possible that earlier volcanic activity in a similar tectonic setting contributed material to the Walloon Coal Measures succession. The exact source of volcanism remains a question for further investigation.

6. Conclusions

The new data from CA-ID-TIMS high-precision U-Pb zircon analysis presented in this paper are among the first precise set of U-Pb depositional ages for the Surat Basin succession on the eastern margin of the basin, significantly improving the understanding of basin evolution and its stratigraphic framework and advancing the calibration of palynozones. The new age data align with the previous findings of Wainman et al., (2015; 2018a; 2018b). The precise isotopic ages from the Carn Brea 3 and River Road 3 boreholes illustrate that the Walloon Coal Measures range from 165.88 ± 0.11 Ma to 158.84 ± 0.05 Ma, overlapping with previous CA-ID-TIMS ages from Wainman et al., (2015; 2018b). Finally, the Taroom Coal Measures are interpreted to have formed over approximately 2 Ma during the Callovian to early Oxfordian and the Juandah Coal Measures formed over approximately 1.2 Ma during the Oxfordian.

The microfossil assemblage, sampled from both the Taroom Coal Measures and the Juandah Coal Measures, fall within APJ4.2, except for a few samples from River Road 3, younger than 159.69 ± 0.03 Ma, that fall within APJ4.3. The biozone of APJ4.3 was not observed in the samples from Carn Brea 3 that are older than 158.85 ± 0.06 Ma. However, it is possible that species from the APJ4.3 and APJ5 biozone may be found upon further investigation. The findings interpreted from the age data at the edge of the Surat Basin support the depositional model of the Walloon Coal Measures being diachronous with the Clarence-Moreton Basin stratigraphic succession.

The accompanying data from spore-pollen microfossils consist of mostly conifers and some ferns, lycopods, bryophytes, derived from freshwater or terrestrial plants that formed in a humid and temperate climate. This observation supports previous finding in other wells (Martin et al., 2013; McKellar, 1998; Wainman et al., 2015). The mudstones sampled were formed in a fluvial floodplain environment, which may have become somewhat stagnant resulting in an increase in green algae at certain time periods. In addition to the predominantly terrestrial environment indicators, there are

trace amounts of acritarch *Michystridium*, which occurs in brackish environments, present in several River Road 3 samples, supporting a potential marine connection.

The zircons dated here are predominantly derived from magmas of intermediate composition. The tectonic setting that the parental magmas formed in was likely to be a continental arc, which is consistent with most of the recent studies.

CRedit authorship contribution statement

K. Sobczak: Conceptualization, Investigation, Methodology, Project administration, Visualization, Writing – original draft, Writing – review & editing. **J. Cooling:** Investigation, Methodology, Visualization, Writing – original draft, Writing – review & editing. **T. Crossingham:** Investigation, Methodology, Visualization, Writing – original draft. **H.G. Holl:** Conceptualization, Investigation, Methodology, Project administration. **M. Reilly:** Conceptualization, Investigation, Methodology, Project administration. **J. Esterle:** Investigation, Validation, Writing – original draft, Writing – review & editing. **J.L. Crowley:** Data curation, Investigation, Validation, Visualization. **C. Hannaford:** Data curation, Investigation. **M.T. Mohr:** Data curation, Validation, Visualization. **Z. Hamerli:** Conceptualization. **S. Hurter:** Conceptualization, Funding acquisition, Project administration, Resources.

Declaration of competing interest

The authors declare the following financial interests/personal relationships which may be considered as potential competing interests: The authors wish to acknowledge affiliation with the Centre for Natural Gas, University of Queensland, which is currently funded by the University of Queensland and the industry members APLNG, Arrow Energy, and Santos. This research has been conducted with the support of the Centre's industry members – APLNG, Arrow Energy, and Santos. We disclose this information as it may be considered as perceived conflict of interest. However, this research was conducted in accordance with the University of Queensland's policies and procedures relating to research conduct and integrity and we declare that no actual conflict of interest exists..

Acknowledgements

We acknowledge the Turrbal and Yuggera peoples, Traditional Custodians of the land on which this research was conducted.

This study was conducted at the University of Queensland Centre for Natural Gas, which is currently funded by the University of Queensland and the industry members APLNG, Arrow Energy, and Santos. This research was funded by the Australian Research Council (ARC) Linkage Project (Grant Reference ID: LP190100106), and supported by the Centre's industry members, with in-kind support from the Queensland Government's Office of Groundwater Impact Assessment (OGIA). The information, opinions and views expressed in this paper do not necessarily represent those of the University of Queensland, the Centre for Natural Gas, its constituent members or associated companies.

Many thanks to Chris Hansen and Berny Parkes at the Exploration Data Centre staff for their technical support; to David Purdy of the Geological Survey of Queensland for assistance determining viability of tuff samples with the use of the Olympus Delta Handheld XRF Analyser; to Bob Nicoll of the Geoscience Australia for assistance in coordinating sample analysis; and to Julie Pearce and Elizabeth Alcantarino at the UQ Centre for Natural Gas for ongoing administrative support. Schlumberger provided access to Techlog software.

Appendix A. Supplementary data

Supplementary data to this article can be found online at <https://doi.org/10.1016/j.gr.2024.04.012>.

References

- Abbink, O.A., 1998. Palynological investigations in the Jurassic of the North Sea Region. LPP Contribution Series 9, 1–191.
- Andrade, C., Sobczak, K., Vasconcelos, P., Holl, H.G., Hurter, S., Allen, C.M., 2023. U-Pb detrital zircon geochronology of the Middle to Upper Jurassic strata in the Surat Basin: New insights into provenance, paleogeography, and source-sink processes in eastern Australia. *Mar. Pet. Geol.* 149, 106122.
- Asmussen, P., Pidgeon, B., Gaede, O., Gust, D., Flottmann, T., 2023. Deciphering a cryptic unconformity in the Surat Basin using high frequency detrital zircon U-Pb geochronology: Insights into basin dynamics on the north-east margin of Gondwana. *Gondwana Res.* 118, 117–134.
- Balme, B.E., 1995. Fossil in situ spores and pollen grains: an annotated catalogue. *Rev. Palaeobot. Palynol.* 87 (2), 81–323.
- Bein, C., 2016. Provenance of the Springbok Sandstone, Surat Basin, Queensland, The University of Queensland, School of Earth Sciences, honours thesis.
- Belousova, E., Griffin, W.L., O'Reilly, S.Y., Fisher, N., 2002. Igneous zircon: trace element composition as an indicator of source rock type. *Contrib. Mineral. Petrol.* 143 (5), 602–622.
- Bianchi, V., Zhou, F., Pistellato, D., Martin, M., Boccardo, S., Esterle, J., 2018. Mapping a coastal transition in braided systems: an example from the Precipice Sandstone, Surat Basin. *Aust. J. Earth Sci.* 65 (4), 483–502.
- Bryan, S., Constantine, A., Stephens, C., Ewart, A., Schön, R., Parianos, J., 1997. Early Cretaceous volcano-sedimentary successions along the eastern Australian continental margin: implications for the break-up of eastern Gondwana. *Earth Planet. Sci. Lett.* 153 (1), 85–102.
- Bryan, S.E., Cook, A.G., Allen, C.M., Siegel, C., Purdy, D.J., Greentree, J.S., Uysal, I.T., 2012. Early-mid Cretaceous tectonic evolution of eastern Gondwana: from silicic IIP magmatism to continental rupture. *Episodes J. Int. Geosci.* 35 (1), 142–152.
- Bryan, S., Ewart, A., Stephens, C., Parianos, J., Downes, P., 2000. The Whitsunday Volcanic Province, Central Queensland, Australia: lithological and stratigraphic investigations of a silicic-dominated large igneous province. *J. Volcanol. Geotherm. Res.* 99 (1–4), 55–78.
- Burke, K., 2011. Plate tectonics, the Wilson Cycle, and mantle plumes: geodynamics from the top. *Annu. Rev. Earth Planet. Sci.* 39, 1–29.
- Cook, A., Bryan, S., Draper, J., 2013. Post-orogenic Mesozoic basins and magmatism. In: *Jell, P.A. (Ed.), Geology of Queensland*. Geological Survey of Queensland, Brisbane, Australia, pp. 515–575.
- Cooling, J.J., Crowley, J.L., McKellar, J.L., Esterle, J.S., Nicoll, R.S., Bianchi, V., 2020. Stratigraphic constraints on the Early Cretaceous Orallo Formation, southeastern Queensland: U-Pb dating of bentonite and palynostratigraphy of associated strata. *Aust. J. Earth Sci.* 68 (3), 343–354.
- Corfu, F., Hanchar, J.M., Hoskin, P.W.O., Kinny, P., 2003. Atlas of Zircon Textures. *Rev. Mineral. Geochemistry* 53, 469–500.
- de Jersey, N.J., 1959. Jurassic spores and pollen grains from the Rosewood Coalfield. *QGMJ* 60, 346–366.
- de Jersey, N.J., 1960. Jurassic spores and pollen grains from the Rosewood Coalfield. *GSQ Publication* 294, 1–14.
- de Jersey, N.J., McKellar, J.L., 2013. The palynology of the Triassic-Jurassic transition in southeastern Queensland, Australia, and correlation with New Zealand. *Palynology* 37 (1), 77–114.
- Exon, N.F., 1976. Geology of the Surat Basin. Queensland, BMR Bulletin, p. 166.
- Exon, N.F., Burger, D., 1981. Sedimentary cycles in the Surat Basin and global changes of sea level. *BMR J. of Aust. Geol. & Geophys.* 6, 153–159.
- Fedo, C.M., Sircombe, K.N., Rainbird, R.H., 2003. Detrital zircon analysis of the sedimentary record. *Rev. Mineral. Geochem.* 53, 277–303.
- Fielding, C.R., 1993. The Middle Jurassic Walloon Coal Measures in the type area, the Rosewood-Walloon Coalfield. *SE Queensland. Australian Coal Geology* 9, 16.
- Fielding, C.R., Kassan, J., Draper, J.J., 1996. Geology of the Bowen and Surat Basins, Eastern Queensland, Springwood. Geological Society of Australia, N.S.W.
- Foley, E.K., Henderson, R.A., Roberts, E.M., Kemp, A.I.S., Todd, C.N., Knutsen, E.M., Fisher, C., Wainman, C.C., Spandler, C., 2021. Jurassic Arc: Reconstructing the Lost World of eastern Gondwana. *Geology* 49 (11), 1391–1396.
- Gaede, O., Levy, M., Murphy, D., Jenkinson, L., Flottmann, T., 2020. Well-log-constrained porosity and permeability distribution in the Springbok Sandstone, Surat Basin, Australia. *Hydrogeol. J.* 28 (1), 103–124.
- Gallagher, K., Dumitru, T.A., Gleadow, A.J.W., 1994. Constraints on the vertical motion of eastern Australia during the Mesozoic. *Basin Res.* 6 (2–3), 77–94.
- Gehrels, G., 2014. Detrital Zircons U-Pb geochronology Applied to Tectonics. *Annu. Rev. Earth Planet. Sci.* 42, 127–149.
- Green, P., Hoffmann, K., Brian, T., Gray, A., Murray, C., Carmichael, D., McKellar, J., Beeston, J., Price, P., Smith, M., 1997. The Surat and Bowen Basins, south-east Queensland. Queensland Department of Mines and Energy, Queensland Minerals and Energy Review Series, p. 238.
- Grimes, C., Wooden, J., Cheadle, M., John, B., 2015. “Fingerprinting” tectono-magmatic provenance using trace elements in igneous zircon. *Contrib. Mineral. Petrol.* 170 (5–6), 1–26.
- Hamilton, S.K., Esterle, J.S., Sliwa, R., 2014. Stratigraphic and depositional framework of the Walloon Subgroup, eastern Surat Basin. Queensland. *Aust. J. Earth Sci.* 61 (8), 1061–1080.
- Helby, R., Morgan, R., & Partridge, A. D., 1987. A palynological zonation of the Australian Mesozoic. In: *Jell, P. A. (Ed.), Studies in Australian Mesozoic palynology* 4, 1–9. Association of Australasian Palaeontologists, Memoir 4.
- Henderson, R., Spandler, C., Foley, E.K., Kemp, A.I.S., Roberts, E.M., Fisher, C., 2022. Early cretaceous tectonic setting of eastern Australia: Evidence from the subduction-related Morton Igneous Association of Southeast Queensland. *Lithos*, 410–411.
- Hentschel, A., 2018. Integrating coal petrology, geochemistry and geochronology to understand spatial variation in the Walloon Subgroup. University of Queensland. PhD Thesis.
- Jell, P.A. (Ed.), 2013. *Geology of Queensland*, Geological Survey of Queensland. Brisbane, Qld.
- Jones, G., Patrick, R., 1981. Stratigraphy and coal exploration geology of the northeastern Surat Basin. *Coal Geol.* 1 (4), 153–163.
- Korsch, R.J., Totterdell, J.M., 2009a. Evolution of the Bowen, Gunnedah and Surat Basins, eastern Australia. *Aust. J. Earth Sci.* 56, 271–272.
- Korsch, R.J., Totterdell, J.M., 2009b. Subsidence history and basin phases of the Bowen, Gunnedah and Surat Basins, eastern Australia. *Aust. J. Earth Sci.* 56 (3), 335–353.
- Korsch, R.J., Totterdell, J.M., Fomin, T., Nicoll, M.G., 2009. Contractual structures and deformational events in the Bowen, Gunnedah and Surat Basins, eastern Australia. *Aust. J. Earth Sci.* 56, 477–499.
- Ludwig, K.R., 2003. *User's Manual for Isoplot 3.00*. Berkeley Geochronology Center: Berkeley, CA, 70 p.
- Martin, M.A., Wakefield, M., MacPhail, M.K., Pearce, T., Edwards, H.E., 2013. Sedimentology and stratigraphy of an intra-cratonic basin coal seam gas play: Walloon Subgroup of the Surat Basin, eastern Australia. *Pet. Geosci.* 19 (1), 21.
- Martin, M., Wakefield, M., Bianchi, V., Esterle, J., Zhou, F., 2018. Evidence for marine influence in the Lower Jurassic Precipice Sandstone, Surat Basin, eastern Australia. *Aust. J. Earth Sci.* 65 (1), 75–91.
- McKellar, J.L., 1998. Late Early to Late Jurassic palynology, biostratigraphy and palaeogeography of the Roma Shelf area, northwestern Surat Basin, Queensland, Australia: including phytogeographic-palaeoclimatic implications of the Callialasporites dampieri and Microcaryidites microfloras in the Jurassic-Early Cretaceous of Australia, based on an overview assessed against a background of floral change and apparent true polar wander in the preceding late Palaeozoic-early Mesozoic. The University of Queensland. PhD Thesis.
- Power, P.E., Devine, S.B., 1970. Surat Basin, Australia—Subsurface Stratigraphy, History, and Petroleum. *AAPG Bull.* 54 (12), 2410–2437.
- Price, P.L., Filatoff, J., William, A.J., Pickering, S.A., Wood, G.R., 1985. Late Palaeozoic and Mesozoic palynostratigraphical units. CSR Oil & Gas Division, Palynology Facility, Report 274, 25 pp.
- Price, P., 1997. Permian to Jurassic Palynostratigraphic Nomenclature of the Bowen and Surat Basins. In: *Green, P. M. (Ed.), The Surat and Bowen Basins, South-East Queensland*. Brisbane, Queensland Department of Mines and Energy 1, 137–178.
- R Core Team, 2023. *R: A Language and Environment for Statistical Computing*. R Foundation for Statistical Computing, Vienna, Austria. <https://www.R-project.org/>.
- Raza, A., Hill, K.C., Korsch, R.J., 2009. Mid-Cretaceous uplift and denudation of the Bowen and Surat Basins, eastern Australia: relationship to Tasman Sea rifting from apatite fission-track and vitrinite-reflectance data. *Aust. J. Earth Sci.* 56 (3), 501–531.
- Ryan, D.J., Hall, A., Erriah, L., Wilson, P.B., 2012. The Walloon coal seam gas play, Surat Basin. *APPEA Journal* 52, 273–290.
- Scott, S., Anderson, B., Crosdale, P., Dingwall, J., Leblang, G., 2007. Coal petrology and coal seam gas contents of the Walloon Subgroup, Surat Basin, Queensland. *Australia. Int. J. Coal Geol.* 70, 209–222.
- Shanley, K.W., McCabe, P.J., 1994. Perspective on the sequence stratigraphy of continental strata. *AAPG Bull.* 78 (4), 544–568.
- Shepherd, M., 2009. Meandering fluvial reservoirs in Oil field production geology. *AAPG Mem.* 91, 161–272.
- Shields, D., Esterle, J.S., 2016. Regional insights into the sedimentary organisation of the Walloon Subgroup, Surat Basin. Queensland. *Aust. J. Earth Sci.* 62, 949–967.
- Shields, D., Bianchi, V., Esterle, J., 2017a. A seismic investigation into the geometry and controls upon alluvial architecture in the Walloon Subgroup, Surat Basin. Queensland. *Aust. J. Earth Sci.* 64 (4), 455–469.
- Shields, D., Zhou, F., Buchannan, A., Esterle, J., 2017b. Complementing coal seam gas facies modelling workflows with decompaction based processes. *Mar. Pet. Geol.* 88, 155–169.
- Sliwa, R., Esterle, J., 2008. Re-evaluation of structure and sedimentary packages in the eastern Surat Basin. Petroleum Exploration Society of Australia, Special Publication.
- Sobczak, K., Holl, H.G., Garnett, A., 2021. Estimating porosity and permeability in the Springbok Sandstone, Surat Basin (Queensland), using new wireline log-based workflow. *APPEA Journal* 61 (2), 720–725.
- Swarbrick, C.F.J., Gray, A.R.G., Exon, N.F., 1973. Injune Creek Group – Amendments and an addition to stratigraphic nomenclature in the Surat Basin. *QGMJ* 74, 57–63.
- Towler, B., Firouzi, M., Underschultz, J., Rifkin, W., Garnett, A., Schultz, H., Esterle, J., Tyson, S., Witt, K., 2016. An overview of the coal seam gas developments in Queensland. *J. Nat. Gas Eng.* 31, 249–271.
- Trayler, R.B., Schmitz, M.D., Cuitiño, J.L., Kohn, M.J., Bargo, M.S., Kay, R.F., Strömberg, C.A.E., Vizcaino, S.F., 2019. An improved approach to age-modeling in deep

- time: Implications for the Santa Cruz Formation, Argentina. *Geol. Soc. Am. Bull.* 132, 233–244.
- Tucker, R.T., Roberts, E.M., Henderson, R.A., Kemp, A.I.S., 2016. Large igneous province or long-lived magmatic arc along the eastern margin of Australia during the Cretaceous? Insights from the sedimentary record. *Geol. Soc. Am. Bull.* 128 (9–10), 1461–1480.
- Wainman, C.C., McCabe, P.J., Crowley, J.L., Nicoll, R.S., 2015. U-Pb zircon age of the Walloon Coal Measures in the Surat Basin, southeast Queensland: implications for paleogeography and basin subsidence. *Aust. J. Earth Sci.* 62 (7), 807–816.
- Wainman, C.C., Hannaford, C., Mantle, D., McCabe, P.J., 2018a. Utilizing U-Pb CA-TIMS dating to calibrate the Middle to Late Jurassic spore-pollen zonation of the Surat Basin, Australia to the geological time-scale. *Alcheringa: an Australasian Journal of Palaeontology* 42 (3), 402–414.
- Wainman, C.C., McCabe, P.J., Crowley, J.L., 2018b. Solving a tuff problem: Defining a chronostratigraphic framework for Middle to Upper Jurassic nonmarine strata in eastern Australia using uranium–lead chemical abrasion–thermal ionization mass spectrometry zircon dates. *AAPG Bull.* 102 (6), 1141–1168.
- Wainman, C.C., McCabe, P.J., 2019. Evolution of the depositional environments of the Jurassic Walloon Coal Measures, Surat Basin, Queensland, Australia. *Sedimentology* 66 (5), 1673–1699.
- Wainman, C.C., Reynolds, P., Hall, T., McCabe, P.J., Holford, S.P., 2019. Nature and origin of tuff beds in Jurassic strata of the Surat Basin, Australia: Implications on the evolution of the eastern margin of Gondwana during the Mesozoic. *J. Volcanol. Geotherm. Res.* 377, 103–116.
- Waschbusch, P., Korsch, R.J., Beaumont, C., 2009. Geodynamic modelling of aspects of the Bowen, Gunnedah, Surat and Eromanga Basins from the perspective of convergent margin processes. *Aust. J. Earth Sci.* 56 (3), 309–334.
- Yago, J.V.R., 1996. Basin analysis of the Middle Jurassic Walloon Coal Measures in the Great Artesian Basin, Australia. University of Queensland. PhD Thesis.
- Yago, J. V., & Fielding, C. R., 2015. Depositional environments and sediment dispersal patterns of the Jurassic Walloon Subgroup in Eastern Australia. Society of Exploration Geophysicists and AAPG International Conference & Exhibition, Melbourne, Victoria, Australia, September 2015, p. 45.
- Zhou, F., Tyson, S., Shields, D., Titheridge, D., Esterle, J.S., 2017. Understanding the geometry and distribution of fluvial channel sandstones and coal in the Walloon Coal Measures, Surat Basin, Australia. *Mar. Pet. Geol.* 86, 573–586.